

MODELLING AND SIMULATION OF DRYING PROCESS FOR CERAMIC  
MEMBRANE FABRICATION

ONG TZE CHING

A thesis submitted in  
fulfillment of the requirement for the award of the  
Doctor of Philosophy

Faculty of Mechanical and Manufacturing Engineering  
Universiti Tun Hussein Onn Malaysia

JULY 2015

## ABSTRACT

For ages, ceramic properties and structure is known for its brittleness and its failure such as cracking and warping. This weakness also relates to the high sensitivity of ceramic to any thermal gradient effects. Therefore, processing steps of green body of ceramic is crucial especially in membrane fabrication that has a multilayer structure to ensure the efficiency of its applications. Thus, every step of ceramic membrane preparation and fabrication needs careful control and monitoring to fulfil these aims. Drying is one of the main problems that is always associated with the cracks and leakages of the ceramic membrane. In fact, the drying process is one of the longest steps corresponding to various evolutions of parameters during the evaporation process. Due to the limitation in experimental or empirical ability to determine the changes of dynamic critical variables during drying, modelling and simulation seems to be the right option to determine and investigate these nonlinear and dynamic variables and will be the focus of this study. This two-dimensional mathematical modelling approach is able to predict the changes of variables in heat and mass transfer during the drying process. The governing system of fully coupled non-linear partial differential equations of the model was derived from a mechanistic approach where the mass and energy conservation laws are defined for a particular phase into which Darcy's law and Fick's law are substituted. A fully implicit algorithm has been employed for numerical solution using the finite element method in which the Galerkin weighted residual method is used in the spatial discretization and a backward finite difference time-stepping scheme is employed for time integration. The ability of this improved model is not restricted to a single homogenous layer of hygroscopic and non-hygroscopic material, but on the novelty to incorporate multilayer heterogeneous material properties as a membrane structure. A good agreement obtained by respective validation works suggested that the model development and implementation are satisfactory. Subsequently, case studies involving single layer and multilayer have produced reasonable accuracy at all times. The application of the model at various case studies involves a convective and enhanced intermittent drying mode which demonstrates the robustness and trustworthiness in predicting and optimising the drying process.

## ABSTRAK

Ciri-ciri dan struktur seramik dikenali dengan sifat kerapuhan dan kegagalannya seperti keretakan dan meleding sejak berzaman lagi. Kelemahan ini juga dikaitkan dengan sensitivitinya terhadap sebarang perubahan haba. Oleh itu, langkah-langkah pemprosesan jasad hijau seramik adalah penting terutamanya dalam fabrikasi membran yang mempunyai pelbagai struktur lapisan dalam memastikan kecekapan aplikasinya. Justeru, langkah-langkah penyediaan dan fabrikasi membran seramik memerlukan kawalan dan pemantauan yang teliti bagi mencapai matlamat tersebut. Pengeringan adalah salah satu masalah utama yang seringkali dikaitkan dengan keretakan dan kebocoran membran seramik. Tambahan pula, proses pengeringan melibatkan tempoh masa yang sangat lama rentetan daripada pelbagai evolusi parameter semasa proses penyejatan. Disebabkan batasan keupayaan eksperimen atau empirikal untuk menentukan perubahan pembolehubah kritikal dinamik semasa pengeringan, pemodelan dan simulasi menjadi pilihan yang betul dalam menentukan dan menyiasat pembolehubah tidak sejajar serta dinamik dan akan menjadi fokus kajian ini. Pendekatan pemodelan matematik dua dimensi ini dapat meramalkan perubahan pembolehubah dalam haba dan pemindahan jisim semasa proses pengeringan. Sistem pengolahan dengan persamaan pembezaan separa bukan linear penuh yang diperoleh daripada pendekatan mekanistik dimana hukum pemuliharaan jisim dan tenaga ditakrifkan untuk fasa tertentu untuk digantikan dengan hukum Darcy dan hukum Fick. Satu algoritma tersirat penuh digunakan untuk penyelesaian berangka yang menggunakan kaedah unsur terhingga dimana kaedah pemberat Galerkin digunakan dalam diskritisasi ruang dan skim perbezaan terhingga masa-loncatan ke belakang digunakan untuk integrasi masa. Kemampuan model ini tidak terhad kepada satu lapisan homogen bahan higroskopik dan bukan higroskopik, tetapi pada keupayaan yang novel dalam menggabungkan sifat heterogen bahan pelbagai lapisan sebagai struktur membran. Satu persetujuan yang baik telah dicapai daripada kerja-kerja pembuktian yang mencadangkan pembangunan dan pelaksanaan model adalah memuaskan. Sejurus itu, kajian kes yang melibatkan lapisan tunggal dan berlapis telah menghasilkan ketepatan yang munasabah pada setiap masa. Aplikasi model dalam pelbagai kajian kes melibatkan pengeringan perolakan serta mod pengeringan sekala yang dimajukan menunjukkan keteguhan dan kebolehpercayaan dalam meramal dan mengoptimumkan proses pengeringan.

## CONTENTS

|   |               |
|---|---------------|
| <b>TITLE</b>  | <b>i</b>      |
| <b>DECLARATION</b>  | <b>ii</b>     |
| <b>DEDICATION</b>   | <b>iii</b>    |
| <b>ACKNOWLEDGEMENT</b>  | <b>iv</b>     |
| <b>ABSTRACT</b>   | <b>v</b>      |
| <b>ABSTRAK</b>  | <b>vi</b>     |
| <b>CONTENTS</b>   | <b>vii</b>    |
| <b>LIST OF TABLES</b>   | <b>xii</b>    |
| <b>LIST OF FIGURES</b>  | <b>xiii</b>   |
| <b>LIST OF ABBREVIATIONS</b>  | <b>xviii</b>  |
| <b>LIST OF SYMBOLS</b>  | <b>xix</b>    |
| <b>LIST OF APPENDICES</b>   | <b>xxiv</b>   |
| <br><b>CHAPTER 1 INTRODUCTION</b>                                   | <br><b>1</b>  |
| 1.1 Research background   | 1             |
| 1.2 Problem statement   | 7             |
| 1.3 Research objective  | 8             |
| 1.4 Scopes  | 8             |
| 1.5 Research contributions  | 9             |
| 1.6 Structure of the thesis   | 10            |
| <br><b>CHAPTER 2 LITERATURE REVIEW</b>                              | <br><b>12</b> |
| 2.1 Introduction  | 12            |
| 2.2 Membrane structure  | 13            |
| 2.3 Preparation of ceramic membrane                                 | 14            |
| 2.4 Importance of drying process in ceramic membrane<br>preparation | 16            |
| 2.5 Drying theory and mechanism of porous structure                 | 17            |

|         |  |    |
|---------|--|----|
| 2.5.1   | Drying period  | 17 |
| 2.5.2   | Kinetic of dynamic drying diffusivity                          | 21 |
| 2.5.3   | Drying in non-hygroscopic and hygroscopic materials            | 22 |
| 2.5.4   | Drying shrinkage   | 23 |
| 2.5.5   | Drying mode: stationary versus intermittent                    | 26 |
| 2.6     | Transport properties of porous material                        | 29 |
| 2.6.1   | Material properties  | 30 |
| 2.6.1.1 | Density  | 30 |
| 2.6.1.2 | Porosity   | 30 |
| 2.6.1.3 | Liquid and vapour permeability                                 | 31 |
| 2.6.1.4 | Thermal conductivity and specific heat                         | 31 |
| 2.6.1.5 | Physical properties of hygroscopic and non-hygroscopic ceramic | 32 |
| 2.6.1.6 | Physical properties of liquid water                            | 33 |
| 2.6.1.7 | Physical properties of gas                                     | 33 |
| 2.6.1.8 | Capillary mechanism  | 34 |
| 2.6.1.9 | Water retention curve  | 35 |
| 2.6.2   | Various transport mechanism in porous media                    | 40 |
| 2.6.2.1 | Darcy flow for liquid due to gas and capillary pressures       | 40 |
| 2.6.2.2 | Darcy flow for gases due to gas pressure                       | 41 |
| 2.6.2.3 | Fick diffusion for vapour flow                                 | 41 |
| 2.6.2.4 | Bound water flow   | 42 |
| 2.6.2.5 | Fourier conduction heat transfer                               | 42 |
| 2.6.2.6 | Convective heat transfer                                       | 43 |
| 2.6.2.7 | Latent heat transfer   | 43 |
| 2.6.2.8 | Dry gas transfer   | 44 |
| 2.7     | Mathematical drying model                                      | 44 |
| 2.8     | Summary  | 48 |

|  |           |
|--|-----------|
| <b>CHAPTER 3 THEORETICAL FORMULATION AND<br/>NUMERICAL METHOD</b>          | <b>50</b> |
| 3.1 Introduction   | 50        |
| 3.2 Limitations and assumptions  | 51        |
| 3.3 Conservation of mass for water flow                                    | 52        |
| 3.4 Conservation of heat transfer  | 61        |
| 3.5 Dry Gas Transfer   | 65        |
| 3.6 Numerical solution   | 67        |
| 3.6.1 Spatial Discretisation using the Finite<br>Element Method            | 68        |
| 3.6.2 Incorporation of Boundary Conditions                                 | 75        |
| 3.6.3 Temporal Discretisation - Time Stepping<br>Algorithms                | 77        |
| 3.7 Algorithm flow chart   | 79        |
| 3.8 Background and model set-up  | 81        |
| 3.8.1 Case 1: Drying study on capillary suction                            | 82        |
| 3.8.2 Case 2: Drying validation with Hall et al.[7]<br>work                | 82        |
| 3.8.3 Case 3: Drying validation with<br>Stanish et al. [46] work           | 83        |
| 3.8.4 Case 4: Drying study on bound water equation                         | 84        |
| 3.8.5 Case 5: Drying validation with<br>Zhang et al. [10] work             | 85        |
| 3.8.6 Case 6: Drying validation with Przesmycki<br>and Strumillo[117] work | 86        |
| 3.8.7 Case 7: Drying study on effect of material<br>parameter sensitivity  | 87        |
| 3.8.8 Case 8: Drying study on drying variables<br>evolution                | 88        |
| 3.8.9 Case 9: Drying validation with Or et al.[102]<br>work                | 89        |
| 3.8.10 Case 10: Drying study on membrane side<br>surface drying            | 90        |

|   |   |            |
|---|---|------------|
| 3.8.11                                  | Case 11: Drying study on membrane top surface drying  | 91         |
| 3.8.12                                  | Case 12: Drying study on stationary drying shrinkage  | 91         |
| 3.8.13                                  | Case 13: Drying validation with Kowalski and Pawlowski [16], [69] work                          | 95         |
| 3.8.14                                  | Case 14: Drying validation with Manel <i>et al.</i> [68] work                                   | 96         |
| 3.8.15                                  | Case 15: Drying study on intermittent drying shrinkage  | 97         |
| 3.8.16                                  | Case 16: Drying study on mesh sensitivity   | 99         |
| <b>CHAPTER 4 RESULTS AND DISCUSSION</b> |   | <b>102</b> |
| 4.1                                     | Introduction  | 102        |
| 4.2                                     | Case 1: Capillary suction for drying of hygroscopic and non-hygroscopic material                | 104        |
| 4.3                                     | Single layer ceramic  | 107        |
| 4.3.1                                   | Drying of non-hygroscopic model   | 107        |
| 4.3.1.1                                 | Case 2: Drying validation with experimental data  | 108        |
| 4.3.1.2                                 | Case 3: Drying validation with experimental data and mathematical model                         | 109        |
| 4.3.2                                   | Drying of hygroscopic model   | 111        |
| 4.3.2.1                                 | Case 4: Bound water equation based on different model   | 111        |
| 4.3.2.2                                 | Case 5: Drying validation with experimental data and mathematical model above irreducible level | 112        |
| 4.3.2.3                                 | Case 6: Drying validation with mathematical model below irreducible level                       | 114        |
| 4.3.3                                   | Case 7: Effect of material parameter sensitivity towards drying patterns                        | 115        |

|       |   |            |
|-------|---|------------|
| 4.3.4 | Case 8: Drying variables evolution for hygroscopic and non-hygroscopic material   | 121        |
| 4.3.5 | Drying diffusivity for hygroscopic and non-hygroscopic material   | 124        |
| 4.4   | Multilayer ceramic: membrane  | 126        |
| 4.4.1 | Case 9: Drying validation with experimental data: drying front movement   | 127        |
| 4.4.2 | Case 10: Drying of side surface   | 129        |
| 4.4.3 | Case 11: Drying of top surface  | 137        |
| 4.4.4 | Case 12: Shrinkage: case study in stationary drying technique   | 144        |
| 4.5   | Intermittent drying technique   | 147        |
| 4.5.1 | Case 13: Drying validation with experimental data and mathematical model: with a varied parameter and a fixed parameter | 148        |
| 4.5.2 | Case 14: Drying validation with mathematical model: varying both parameters   | 150        |
| 4.5.3 | Case 15: Shrinkage: case study in intermittent drying technique   | 152        |
| 4.6   | Case 16: Mesh sensitivity: coarse and finer mesh domain   | 156        |
| 4.7   | Summation of results  | 164        |
|       | <b>CHAPTER 5 CONCLUSIONS AND RECOMMENDATIONS</b>  | <b>165</b> |
| 5.1   | Conclusions   | 165        |
| 5.2   | Recommendations   | 166        |
|       | <b>REFERENCES</b>   | <b>168</b> |
|       | <b>APPENDIX A</b>   | <b>181</b> |



**LIST OF TABLES**

|     |  |    |
|-----|--|----|
| 2.1 | Physical properties of hygroscopic and non-hygroscopic ceramic | 33 |
| 2.2 | Physical properties of liquid water                            | 33 |
| 2.3 | Physical properties of vapour and air                          | 34 |
| 2.4 | Fitting parameters in VG equation [83]                         | 40 |
| 3.1 | Fitting parameters in VG equation                              | 82 |
| 3.2 | Physical properties of the brick material                      | 86 |
| 3.3 | Physical properties of ceramic body and transport parameter    | 89 |
| 3.4 | Material properties of a clay material                         | 92 |
| 3.5 | Material properties  | 95 |
| 3.6 | Physical properties of the Bentonite material                  | 96 |

## LIST OF FIGURES

|     |  |    |
|-----|--|----|
| 1.1 | Several stages in removal of water from between clay particles during the drying process. (a) Wet body. (b) Partially dry body. (c) Completely dry body [11] | 3  |
| 1.2 | Schematic diagram of the drying of a ceramic green body showing the weight loss and shrinkage with time [12]   | 4  |
| 1.3 | Warpage from drying a tile [13]  | 5  |
| 1.4 | Contribution of current work {the insert figure is contribution of previous work}  | 10 |
| 2.1 | SEM micrograph of layered ceramic membrane [1]   | 13 |
| 2.2 | Schematic representation of an asymmetric membrane [1]   | 14 |
| 2.3 | Three step procedure for ceramic membranes [1]   | 15 |
| 2.4 | Schematic view of phase exists in a porous medium [23]   | 17 |
| 2.5 | A typical moisture content profile. (A) Warm-up period. (B) Constant rate period. (C) First falling rate period. (D) Second falling rate period. [37]        | 18 |
| 2.6 | Drying model [10]  | 20 |
| 2.7 | Variations of effective diffusivity with moisture content [43]   | 22 |
| 2.8 | Volume shrinkage and drying rate of a ceramic body [62]  | 25 |
| 2.9 | Schematic drawing of ceramic crack initiation process. (a) Initial fully saturated matrix. (b)   | 25 |

|      |  |     |
|------|--|-----|
|      | Water–air interface meniscus developed between particles. (c) Tensile stress developed in the upper layer. (d) Surface crack initiated.[63]                            |     |
| 2.10 | WRC for soils of different texture [79]  | 37  |
| 3.1  | Eight-node quadratic quadrilateral element[95]   | 70  |
| 3.2  | Overall model setup  | 80  |
| 3.3  | Detail setup of AX   | 81  |
| 3.4  | Mesh sample of the slab  | 88  |
| 3.5  | Mesh of the ceramic membrane   | 90  |
| 3.6  | Measured volume shrinkage results from experiment for constant rate period   | 93  |
| 3.7  | Measured volume shrinkage results from experiment for falling rate period  | 93  |
| 3.8  | Mesh of the slab   | 94  |
| 3.9  | Intermittent drying configuration condition 1 (denoted as Bi)  | 98  |
| 3.10 | Intermittent drying configuration condition 2 (denoted as Bii)   | 98  |
| 3.11 | Domain used for single layer ((a),(b)), two layers ((c),(d)) and fine interlayer (e)   | 100 |
| 4.1  | Water retention curve: (a) comparison between hygroscopic, non-hygroscopic and reference; (b) comparison of clay and sand {the insert Figure is typical WRC from [70]} | 104 |
| 4.2  | Sample plots: (a) with $n = 0.6$ and $m = 2$ ( $\rho$ varies); (b) with $m = 2$ and $\rho = 46$ ( $n$ varies); (c) with $n = 0.6$ and $\rho = 46$ ( $m$ varies)        | 106 |
| 4.3  | Drying curve   | 109 |
| 4.4  | Saturation curve   | 109 |
| 4.5  | Temperature curve  | 110 |
| 4.6  | Saturation curve for both model  | 112 |
| 4.7  | Drying curve   | 113 |
| 4.8  | Drying curve   | 114 |

|      |   |     |
|------|---|-----|
| 4.9  | Water pressure distribution as a function of depth and time; slab X, b) slab Y, c) slab Z   | 116 |
| 4.10 | Gas pressure distribution as a function of depth and time; a) slab X, b) slab Y, c) slab Z  | 118 |
| 4.11 | Water saturation distribution as a function of depth and time; a) slab X, b) slab Y, c) slab Z  | 120 |
| 4.12 | Pore water pressure distribution as a function of time  | 123 |
| 4.13 | Temperature distribution as a function of time  | 123 |
| 4.14 | Gas pressure distribution as a function of time   | 124 |
| 4.15 | Variations of diffusivity with time. (a) Vapour diffusivity. (b) Bound water diffusivity. (c) Liquid diffusivity  | 125 |
| 4.16 | (a) Initial condition for generated by current model. (b) Saturation contour after 7 hours by current model. (c) Initial condition of drying front from experiment by Or et al [102]. (d) Drying front movement after 7 hours by experiment by Or et al [102] | 128 |
| 4.17 | Movement of drying from the top surface   | 129 |
| 4.18 | Saturation contour at drying times of (a) 0 hour, (b) 1 hour, (c) 2 hours, (d) 3 hours, (e) 4 hours (f) 5 hours 20 min  | 130 |
| 4.19 | Pore gas pressure contour at drying times of (a) 0 hour, (b) 1 hour, (c) 2 hours, (d) 3 hours, (e) 4 hours (f) 5 hours 20 min   | 132 |
| 4.20 | Temperature contour at drying times of (a) 0 hour, (b) 1 hour, (c) 2 hours, (d) 3 hours, (e) 4 hours (f) 5 hours 20 min   | 134 |
| 4.21 | Pore water pressure contour at drying times of (a) 0 hour, (b) 1 hour, (c) 2 hours, (d) 3 hours, (e) 4 hours (f) 5 hours 20 min   | 135 |

|      |  |     |
|------|--|-----|
| 4.22 | Variations of diffusivity with time for multilayer system. (a) Liquid diffusivity. (b) Vapour diffusivity                                    | 137 |
| 4.23 | Pore water pressure distribution as a function of depth and time (a); pore pressure water at 1hour (b); 10hours (c)                          | 138 |
| 4.24 | Temperature distribution as a function of depth and time (a); temperature at 1hour (b); 10hours (c)  | 140 |
| 4.25 | Gas pressure distribution as a function of depth and time (a); gas pressure at 1hour (b); 10hours (c)  | 141 |
| 4.26 | Saturation distribution as a function of depth and time (a); saturation at 1hour (b); 10hours (c)  | 142 |
| 4.27 | Difference in moisture as a function of time   | 144 |
| 4.28 | Volume shrinkage as a function of time; (a) hygroscopic layer, (b) non-hygroscopic layer, (c) differential                                   | 146 |
| 4.29 | Drying shrinkage as a function of time; (a) hygroscopic layer, (b) non-hygroscopic layer, (c) differential                                   | 147 |
| 4.30 | Temperature distribution   | 149 |
| 4.31 | Saturation distribution  | 149 |
| 4.32 | Temperature distribution   | 150 |
| 4.33 | Saturation distribution  | 150 |
| 4.34 | Temperature evolution  | 151 |
| 4.35 | Saturation evolution   | 151 |
| 4.36 | (a) Volume shrinkage as a function of time; (b) differential in volume shrinkage; (c) drying shrinkage; (d) differential in drying shrinkage | 152 |
| 4.37 | (a) Volume shrinkage as a function of time; (b) differential in volume shrinkage; (c) drying shrinkage; (d) differential in drying shrinkage | 154 |

|      |  |     |
|------|--|-----|
| 4.38 | Dimensionless moisture gradient in solid matrix<br>(a) hygroscopic layer (denoted as 1) (b) non-<br>hygroscopic layer (denoted as 2)   | 155 |
| 4.39 | Comparison of saturation level at 0<br>seconds((a),(b)), 30 minutes((c),(d)), 1<br>hour((e),(f)), 4 hours((g),(h)) and 8 hours((i),(j))<br>for both meshes                                   | 157 |
| 4.40 | Comparison coarse and fine mesh saturation<br>evolution at node 22(fine) and 12(coarse) over 8<br>hour drying time for single layer structure.   | 159 |
| 4.41 | Comparison of saturation level at 0<br>seconds((a),(b)), 30 minutes((c),(d)), 1<br>hour((e),(f)), 4 hour((g),(h)) and 8 hour((i),(j)) for<br>both meshes.                                    | 160 |
| 4.42 | Comparison of saturation loss between fine mesh<br>and coarse mesh at node 22, 54(fine) and 12,<br>29(coarse) over 8 hour drying time for two layer<br>structure.                            | 162 |
| 4.43 | Difference in saturation and temperature for<br>interlayer at node 82, 92 and 102 (fine interlayer);<br>18, 23 and 28(coarse interlayer) over 8 hour<br>drying time for two layer structure. | 163 |

**LIST OF ABBREVIATIONS**

|      |   |
|------|---|
| A    | Sample A                                    |
| AEV  | Air entry value                             |
| AX   | 'Main' part of the flow chart in Figure 3.2 |
| B    | Sample B                                    |
| BC   | Brook-Corey                                 |
| C    | Sample C                                    |
| diff | Differential                                |
| h    | Hours                                       |
| hg   | Hygroscopic                                 |
| i    | Intermittent drying setup as in Figure 3.9  |
| ii   | Intermittent drying setup as in Figure 3.10 |
| mins | Minutes                                     |
| nhg  | Non-hygroscopic                             |
| WRC  | Water retention curve                       |
| VG   | Van Genuchten                               |
| 1    | Top layer                                   |
| 2    | Support layer                               |

## LIST OF SYMBOLS

|                      |  |                                   |
|----------------------|--|-----------------------------------|
| $a$                  | Coefficient in equation (2.12)               | $\text{N/m}\cdot\text{K}$         |
| $b$                  | Coefficient in equation (2.12)               | $\text{N/m}\cdot\text{K}$         |
| $C$                  | Concentration of moisture content            | -                                 |
| $C_{ga}$             | Molar concentration of dry air               | $\text{mol m}^{-3}$               |
| $C_{pga}$            | Specific molar heat capacity of dry-air      | $\text{J mol}^{-1} \text{K}^{-1}$ |
| $C_{pl}$             | Specific heat capacity of liquid water       | $\text{J kg}^{-1} \text{K}^{-1}$  |
| $C_{pv}$             | Specific molar heat capacity of water vapour | $\text{J kg}^{-1} \text{K}^{-1}$  |
| $C_{ps}$             | Specific heat capacity of ceramic solid      | $\text{J kg}^{-1} \text{K}^{-1}$  |
| $\underline{C}$      | Defined in equation (3.91)                   |                                   |
| $\underline{C}_{ij}$ | Capacity coefficient                         |                                   |
| $D$                  | Parameter in equation (2.23)                 | -                                 |
| $D_{atm}$            | Molecular diffusivity                        | $\text{m}^2/\text{s}$             |
| $D_{BT}$             | Diffusion coefficient of bound liquid        | $\text{m}^2/\text{s}$             |
| $H$                  | Heat capacity of ceramic                     | $\text{J m}^{-3} \text{K}^{-1}$   |
| $\bar{H}$            | Heat content of ceramic                      | $\text{J m}^{-3}$                 |
|                      | Volumetric rate of evaporation               | $\text{m}^3/\text{s}$             |
| $\underline{J}$      | Defined in equation (3.92)                   |                                   |
| $\underline{J}_m$    | Total moisture flux                          | $\text{kg m}^{-2} \text{s}^{-1}$  |



|                      |  |                      |
|----------------------|--|----------------------|
| $k$                  | Permeability                             | $m^2$                |
| $k_i$                | Intrinsic permeability of ceramic        | $m^2$                |
| $k_{eff}$            | Thermal conductivity                     | $W m^{-1} K^{-1}$    |
| $K_g$                | Gas permeability                         | $m^2 Pa^{-1} s^{-1}$ |
| $k_{rg}$             | Relative gas permeability of ceramic     | -                    |
| $k_{rl}$             | Relative hydraulic conductivity          | -                    |
| $K_l$                | Saturated hydraulic conductivity         | $s^{-1}$             |
| $\underline{K}$      | Defined in equation (3.90)               |                      |
| $\underline{K}_{ij}$ | Kinetic coefficients                     |                      |
| $L$                  | Latent heat of vaporisation              | $J kg^{-1}$          |
| $M$                  | Moisture content                         | -                    |
| $M_a$                | Molar mass for air                       | $g/mol$              |
| $M_v$                | Molar mass for vapour                    | $g/mol$              |
| $m$                  | van Genuchten coefficient                | -                    |
| $n$                  | van Genuchten coefficient                | -                    |
| $N_r$                | Shape function of residual error         | -                    |
| $N_s$                | Shape function of system variables       | -                    |
| $P_g$                | Total gas pressure                       | $Pa$                 |
| $P_{gs}$             | Nodal values of total gas pressure       | $Pa$                 |
| $\hat{P}_g$          | Approximate values of total gas pressure | $Pa$                 |
| $P_l$                | Pressure of pore-water                   | $Pa$                 |
| $P_{ls}$             | Nodal values of pore-water pressure      | $Pa$                 |

|                   |   |                                     |
|-------------------|---|-------------------------------------|
| $\hat{P}_l$       | Approximate values of pore-water pressure | Pa                                  |
| q                 | Heat source                               | W/m <sup>2</sup>                    |
| q <sub>b</sub>    | Mass flux for bound water                 | Kg/m <sup>2</sup> s                 |
| q <sub>cond</sub> | Conduction heat flux                      | W/m <sup>2</sup>                    |
| q <sub>conv</sub> | Convection heat flux                      | W/m <sup>2</sup>                    |
| q <sub>L</sub>    | Latent heat flux                          | W/m <sup>2</sup>                    |
| q <sub>l</sub>    | Mass flux for liquid                      | Kg/m <sup>2</sup> s                 |
| q <sub>g</sub>    | Mass flux for gas                         | Kg/m <sup>2</sup> s                 |
| q <sub>ga</sub>   | Mass flux for dry gas                     | Kg/m <sup>2</sup> s                 |
| q <sub>v</sub>    | Mass flux for vapour                      | Kg/m <sup>2</sup> s                 |
| R <sub>v</sub>    | Gas constant for water vapour             | J kg <sup>-1</sup> K <sup>-1</sup>  |
| R                 | Universal gas constant                    | J mol <sup>-1</sup> K <sup>-1</sup> |
| r                 | Relative humidity                         | %                                   |
| S <sub>g</sub>    | Degree of gas saturation                  | -                                   |
| S <sub>l</sub>    | Degree of water saturation                | -                                   |
| t                 | Time                                      | s                                   |
| T                 | Temperature                               | K                                   |
| Th                | Temperature                               | °C                                  |
| T <sub>r</sub>    | Reference temperature                     | K                                   |
| T <sub>s</sub>    | Nodal values of total temperature         | K                                   |
| $\hat{T}$         | Approximate values of temperature         | K                                   |
| V <sub>g</sub>    | Average velocity of gas                   | m s <sup>-1</sup>                   |

|            |                            |                    |
|------------|----------------------------|--------------------|
| $V_l$      | Velocity of liquid         | $m s^{-1}$         |
| $V_0$      | Initial volume             | $m^2$              |
| $V_t$      | Final volume               | $m^2$              |
| $V_v$      | Velocity of water vapour   | $m s^{-1}$         |
| $x$        | Global co-ordinates        | $m$                |
| $y$        | Global co-ordinates        | $m$                |
| $z$        | Global co-ordinates        | $m$                |
| $Z$        | elevation head             | $m$                |
| $\alpha$   | van Genuchten coefficient  | -                  |
| $\beta$    | Defined in equation (3.10) | $kg m^{-3} K^{-1}$ |
| $\gamma_1$ | Constant in equation (2.1) | -                  |
| $\gamma_2$ | Constant in equation (2.1) | -                  |
| $\xi$      | Local co-ordinate          | $m$                |
| $\eta$     | Local co-ordinate          | $m$                |
| $\Gamma^e$ | Element boundary surface   | -                  |
| $\theta$   | Volumetric water content   | -                  |
| $\theta_a$ | Volumetric dry-air content | -                  |
| $\theta_l$ | Volumetric liquid content  | -                  |
| $\theta_v$ | Volumetric vapour content  | -                  |
| $r$        | Residual water contents    | -                  |
| $s$        | Saturated water contents   | -                  |
|            | Pore size distribution     | -                  |

|                          |                                       |                                 |
|--------------------------|---------------------------------------|---------------------------------|
| $\lambda_a$              | Thermal conductivity of dry-air       | $\text{W m}^{-1} \text{K}^{-1}$ |
| $\lambda_s$              | Thermal conductivity for solid matrix | $\text{W m}^{-1} \text{K}^{-1}$ |
| $\lambda_l$              | Thermal conductivity of liquid water  | $\text{W m}^{-1} \text{K}^{-1}$ |
| $\lambda_v$              | Thermal conductivity of water vapour  | $\text{W m}^{-1} \text{K}^{-1}$ |
| $\mu_a$                  | Dynamic viscosity of dry-air          | $\text{N s m}^{-2}$             |
| $\mu_v$                  | Dynamic viscosity of water vapour     | $\text{N s m}^{-2}$             |
| $b$                      | Matrix potential at air entry         | Pa                              |
| $(T)$                    | Matrix potential                      | Pa                              |
| $v$                      | Mass flow factor                      | -                               |
| $\rho_l$                 | Liquid water density                  | $\text{kg m}^{-3}$              |
| $\rho_o$                 | Density of saturated vapour           | $\text{kg m}^{-3}$              |
| $\rho_s$                 | Density of ceramic                    | $\text{kg m}^{-3}$              |
| $\rho_v$                 | Density of water vapour               | $\text{kg m}^{-3}$              |
| $\phi$                   | Porosity                              | -                               |
| $\underline{\Phi}$       | Defined in equation (3.93)            |                                 |
| $\dot{\underline{\Phi}}$ | Defined in equation (3.94)            |                                 |
| $\Omega^e$               | Element domain                        |                                 |
| $\omega$                 | Relaxation factor                     | -                               |
| $\varpi$                 | Required time interval                |                                 |

**LIST OF APPENDICES**

| <b>APPENDIX</b> | <b>TITLE</b>           | <b>PAGE</b> |
|-----------------|------------------------|-------------|
| A               | Brook-Corey saturation | 181         |

## **CHAPTER 1**

### **INTRODUCTION**

#### **1.1 Research background**

Membrane technology is an emerging interdisciplinary technology. Its application has produced a significant change since 1960 as it is not only used in laboratory tools but also on industrial sides. Membrane processes have become an accepted unit operation for a variety of separations in industries for various purposes such as gas separation, reverse osmosis, nanofiltration, ultrafiltration, microfiltration, dialysis, reactors, contractors and others [1]. With increasing demand at 9% annual rate [2] especially in water and wastewater industry, new technologies and new processing techniques on membrane production are constantly being discovered and invented. Since membrane technologies are energy intensive, defect-free and quality final products are essential to the applications of membranes in the industry field. Thus, a good understanding of all of the membrane fabrication steps is vital.

Generally, the membrane fabrication process starts from powder formation of the right material combinations. Then it is in the form of slurry or paste to be ready for various ceramic membranes preparation techniques such as slip casting, tape casting, extruding or pressing. Before the precursor formulation forms into the final products, it needs to be dried. The different moisture gradient in this segregated membrane structure will definitely create a difference in thermal gradient effect during the drying process[3]. Eventually, the process will end with the consolidation of membrane by a heat treatment procedure at high temperature. As can be noticed, the drying step will crucially determine the quality of the product before the final consolidation stage. The consequences of improper drying process can lead to the initiation of defects and eventually these defects will continue to propagate, causing undesired failure of the

dried product. On top of that, the drying step is essential for ceramic membrane as this component is a porous structure that consists of a unique separation structure with a multilayer system which leads to a different moisture gradient.

Drying is widely applied in industries such as food, textile, paper, wood, ceramics, minerals, wastewater sludge, pharmaceutical products or biotechnological products [4]. Most of the drying industry uses a convective mechanism as it is more flexible and has low energy consumption [5]. However, the losses due to convective drying defects alone can be up to the order of 10% in industrial production [6]. Hence, optimisation of the drying process in terms of energy usage and production time, without compromising the defects of the product quality such as cracking or warping, requires a comprehensive study and good understanding of the controlling parameters that evolve during the drying process. Generally, drying means the transfer of liquid (normally water) from the pores of a solid material to the surrounding air [7], [8]. Basically, are several stages in removing the water from a solid to the surrounding air as shown in Figure 1.1. The initial wet body evaporates from the drying surface at a constant rate corresponding to liquid flux. The evaporation rate is similar to that from an open dish of liquid where there is a continuous supply of water from the interior of the solid matrix to the evaporation surface [9]. As drying progresses, the fraction of the wet area at the surface decreases with a decreasing open dish liquid. When the water content reaches critical free water content, the surface evaporation will form discontinued wet patches. Thus, this stage of drying has a decreasing evaporation rate while the interior free water supply to the evaporation surface is restrained by the decrease of the free water content. Eventually, the drying surface will recede into the interior of the solid matrix, dividing the solid matrix into two regions, a wet region and a dry region [10]. During this stage, vapour flux substitutes the previous liquid flux as a dominant driving force for moisture transfer. Finally, as drying proceeds, the water content decreases gradually to zero and subsequently vapour flux slows down and decays toward the atmosphere as internal vapour pressure and external vapour pressure is almost in equilibrium. This indicates the end of the drying process.

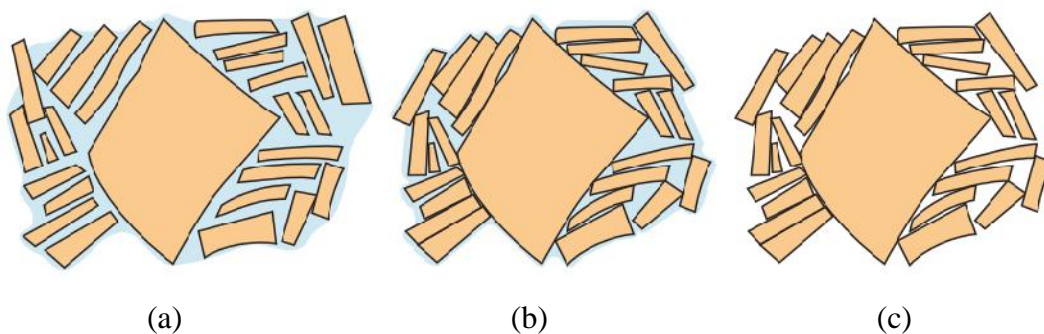


Figure 1.1: Several stages in removal of water from between clay particles during the drying process. (a) Wet body. (b) Partially dry body. (c) Completely dry body [11]

Accordingly, there are various mechanisms and controlling variables corresponding to different stages of the drying period that occur concurrently for moisture evaporation to happen. Thus, it is necessary to carefully control the decisive factors in the drying process in order to avoid defects in the dried product. Unfortunately, drying is often associated with common failures due to improper control of the drying process, such as cracking and warping. Those defects are closely attributed to the non-uniform shrinkage mechanism that happens during the drying process. Figure 1.2 illustrates the progress of the drying green body shrinkage with respect to the weight loss and drying time. In the early stage of the drying process, the moisture weight decreases at a constant rate. Thus the drying rate is at a constant rate and this period of drying is often called the constant rate period. During this period, the surface of the green body is always wet by the flow of liquid to the surface as a consequence of the rearrangement of particles in the green body attributed to the compressive capillary pressure at the surface of the green body. This phenomenon is corresponding to the shrinkage and deformation of the solid as particles come into contact to maintain an expelling of liquid flow to the surface at a constant rate [6]. Subsequently, the drying reaches the decreasing drying rate period when the liquid-vapour interface starts to recede into the solid matrix. During this period, shrinkage is limited when the particles come into contact with liquid filling the pores. Eventually, drying will slow down and end when the moisture content inside the matrix and external surroundings is at the equilibrium state.



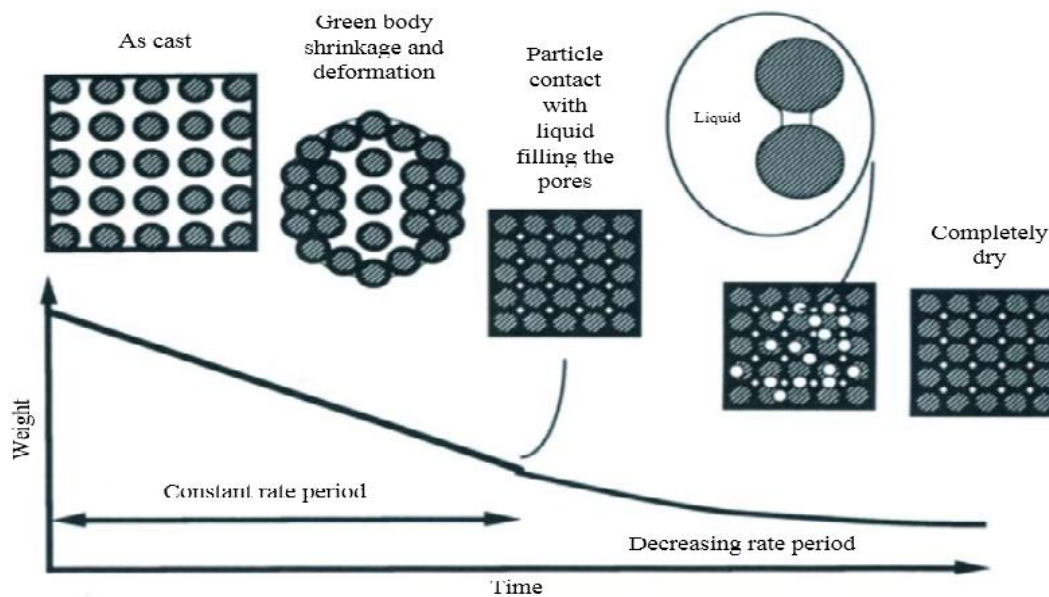


Figure 1.2: Schematic diagram of the drying of a ceramic green body showing the weight loss and shrinkage with time [12]

Cracking is a defect that attributes to the shrinkage phenomenon. Severe cracking could lead to fracture of the material particularly in brittle materials such as ceramic. Critical free moisture content is the initiation point of the cracking mechanism where shrinkage is restricted as particles are closely in contact with each other. The formation of the wet and dry regions in the matrix body eventually causes non-uniform shrinkage on the upper and lower cores of the solid body. The non-uniform shrinkage induces a non-homogeneous drying stress in the solid matrix. Once the drying stress exceeds the maximum tensile strength of the material, surface cracking is likely to happen. Meanwhile, warping often occurs when drying involves one surface drying only as this generates uneven shrinkage. Figure 1.3 demonstrates the warping phenomenon during the drying process of tile. When the drying starts, the upper face dries up faster and creates tensional force caused by compression of the particles. This causes the tile to curl up when the upper face is smaller than the lower face. Upon entering the late stage of drying, the liquid retreats into the solid, and the drying process will be completed. The dry curls remain as the body is too rigid to completely straighten out. Thus, improper control of the drying process can cause non-uniform shrinkage, resulting in failure of the dried product. These defects can be avoided by obtaining a better understanding of the underlying physics of the drying process at a fundamental level via a better configuration of the drying process.

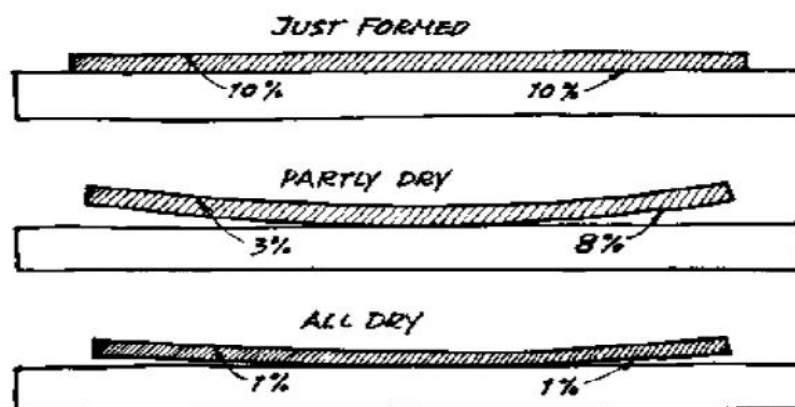


Figure 1.3: Warpage from drying a tile [13]

As has been emphasised earlier, an understanding of the drying process is essential to produce quality defect-free products. The drying phenomenon of moist porous solids is a complicated process involving simultaneous, coupled mass and heat transfer phenomena. Accordingly, drying behaviour can be influenced by a large variety of independent factors, such as ambient conditions, air velocity, relative humidity and saturation as well as material properties such as density, porosity, permeability, hygroscopic and others. Therefore, extensive characterisation of drying behaviour using a strictly experimental approach constitutes a formidable challenge due to the excessively large number of variables that must be considered. However, the task becomes more manageable nowadays with the help of a reliably realistic computational modelling of the drying phenomenon.

The advanced computational modelling is an evolutionary step in pushing the conventional drying process towards optimisation, conceptualisation or designing the next generation drying process. In past decades, computational methods in drying process engineering have been in emerging trend, motivated by its several advantages [14]. Computational modelling seems to be the most convenient method due to its low cost, speed, complete information, the ability to simulate realistic and actual conditions, and ability to simulate ideal conditions [15], [16]. Additionally, simulations lead to deeper physical insight by actually having virtual sensors in nearly each point (using computational meshing). As such, the information on distribution and evolution of all variables within the product can easily be determined, which can feed new ideas for designing or optimising drying processes [14]. Furthermore, modelling has the ability to measure or determine small changes and also has no limitation with respect to the drying conditions and duration. Also to be noted is the

fact that accurate predictions of computational modelling is essential in many engineering applications; one example being optimisation of industrial drying processes with respect to energy and time consumption and product quality [6], [16]–[18]. For that reason, computational modelling has a large potential in both the research level and in the industrial context to develop the next-generation sustainable and green drying technology.

Essentially, the ceramic industry contributes about 10-25% of the national energy consumption for industrial processes [4], [14]. Drying constitutes an essential and energy-intensive unit operation, as most ceramics require drying of at least a part of the product at some stage during processing. Due to these reasons, any initiative work devoted to improve the ceramic drying operation, via saving energy, improving product quality as well as reducing the environmental effect, would be most welcomed and appreciated. Therefore, the computational modelling approach towards this aim has indeed flourished over recent years. However, modelling the most perplexing problems of the ceramic industry are amongst the most challenging in computational modelling, attributed to their complexity, large range of multi-physics transport processes that occur during drying, and their inherent large material characteristic variability. The multi-physics transport and exchange processes involve the coupled heat and mass occurring simultaneously inside the material and also with the environment. Thus, a unique modelling approach must be based on fundamental heat and mass transfer relationships and thermodynamic equilibrium applied on desired drying techniques and specified materials of interest. This provides a tool that is effective in predicting drying behaviour and is also useful in exploring and understanding the impact of important variables in the drying process. In this way, the impact of the many variables on the drying behaviour for a specific material of interest and applied drying technique can be examined and interpreted without having to resort to an extensive program of experimental testing. Additionally, this mathematical modelling normally results in a set of governing equations which need to be numerically solved using a specialized solver and an adaptive mesh scheme. Subsequently, comparisons of model predictions with experimental drying data will then help to verify the drying model.

Despite substantial efforts being devoted to the mathematical modelling of drying phenomenon, the science remains far from perfect and therefore, interest in the subject remains intense and widespread. Many of the previous approaches have been

limited to specific applications with regards to either the material being dried or the particular drying regime or mechanism at work. The lack of carefully obtained experimental data, primarily due to the often complicated nature of the process and the difficulty of making the necessary detailed measurements, is currently hampering the development of the model for the drying process in membrane fabrication. It is quite possible that perhaps the numerical predictions are almost as reliable as experimental data. Hence, the motivation of this study is devoted to develop a tool to simulate drying behaviour of ceramic materials and subsequently allow it to be extended to the fabrication of ceramic membrane. Furthermore, the proposed model is enhanced to accommodate an improved intermittent convective drying technique.

## **1.2 Problem statement**

Fabrication of ceramic porous membrane is very complex and crucial since it involves the development of very thin and dense layers which act as separators in the multilayer structure. Failure to produce defect-free membrane will lead to the failure of the filtering mechanism, especially when the top surface layer is the decisive factor to ensure the perfect functionality of the membrane separation processes. In fabricating a good quality solid porous membrane from the slurry or loose ceramic particles, the drying stages play an important role (besides the other processing parameters). Based on previous studies, most of the failures in the ceramic structure and component are exhibited during different drying stages due to the stresses caused by various gradient effects [12], [19], [20]. Further complications arise when drying involves materials in a multilayer structure that exhibits different drying behaviour. Basically, this is influenced by the shrinkage mechanism as the water removes from the porous structure network in the ceramic body. Hence, it is crucial to control the drying process and this can be achieved by having a better understanding of the dynamic behaviour of the underlying physics during the process for each stage at a fundamental level. With this focus in mind, the experimental approach (uncertainty in dynamic measured results can be as high as 115% [21]) seems to have limited ability for materials with a wide range of interest. Therefore, the development of a mathematical model for the purpose of computational method will provide sufficient generality to evaluate drying processes in the multilayer structure of ceramic materials.

### **1.3 Research objective**

Motivated by the outline problem statement, this present research effort was undertaken with the following objectives:

- i. To develop and establish a theoretical formulation model that integrates hygroscopic and non-hygroscopic material properties with governing equations to investigate the transport variables and mechanisms in drying phenomena for stationary and non-stationary (intermittent) drying techniques that accommodate single layer structure and multilayer structure of the membrane.
- ii. To determine and investigate the most relevant saturation curve for hygroscopic and non-hygroscopic materials which are integrated with critical material properties in establishing drying for ceramic membrane.
- iii. To implement a numerical solution towards fully coupled theory integrated with Finite Element Analysis (FEA) in predicting the variation of critical and measured parameters during the drying process of the ceramic membrane.
- iv. To validate and simulate the theoretical formulation model developed by FORTRAN source code that integrates with all the variables and material properties based on the particular cases of the proposed drying ceramic membrane.

### **1.4 Scopes**

The model was constructed based on drying theories with basic fundamental physical laws as given in the relevant literature on the convective drying technique. The utilisation of the derived relationships requires knowledge of the properties and characteristics of the material to which the analysis will be applied. In spite of the uncertainties associated with ceramic material, it has become an acceptable procedure for most practical problems to approximate ceramic properties for the development of models and analysis. This assumption is corroborated by various models in literature. Eventually, the simulations can be used to identify key model parameters so that

subsequent sensitivity studies can be carried out in order to establish the effects these parameters have on the performance of convective drying.

## **1.5 Research contributions**

This model is developed based on a continuum approach to provide a systematic way to incorporate fully coupled heat, mass and gas transport equations for convective and diffusive mechanisms. The main working parameters in the derivation of the transport equations are temperature, gas pressure and pore water pressure. The initial contribution involves the introduction of bound water flux into the mass conservation equation, coupled with heat and gas transfer as derived in the proposed model for hygroscopic material. Further extension was conducted in this work by developing and applying a comprehensive model that can be used not only in a single layer or homogenous multilayer structure but also in a heterogeneous multilayer structure. This model is also able to accommodate the materials selection of heterogeneous physical properties besides the hygroscopic and non-hygroscopic behaviours which is not established in previous work (insert figure in Figure 1.4). Furthermore, this model is successfully implemented in both stationary and intermittent convective drying techniques. Figure 1.4 demonstrates the simplified contributions of the current model when compared with previous work. The numerical simulation was benchmarked against various results computed by other models and experimental results gained.

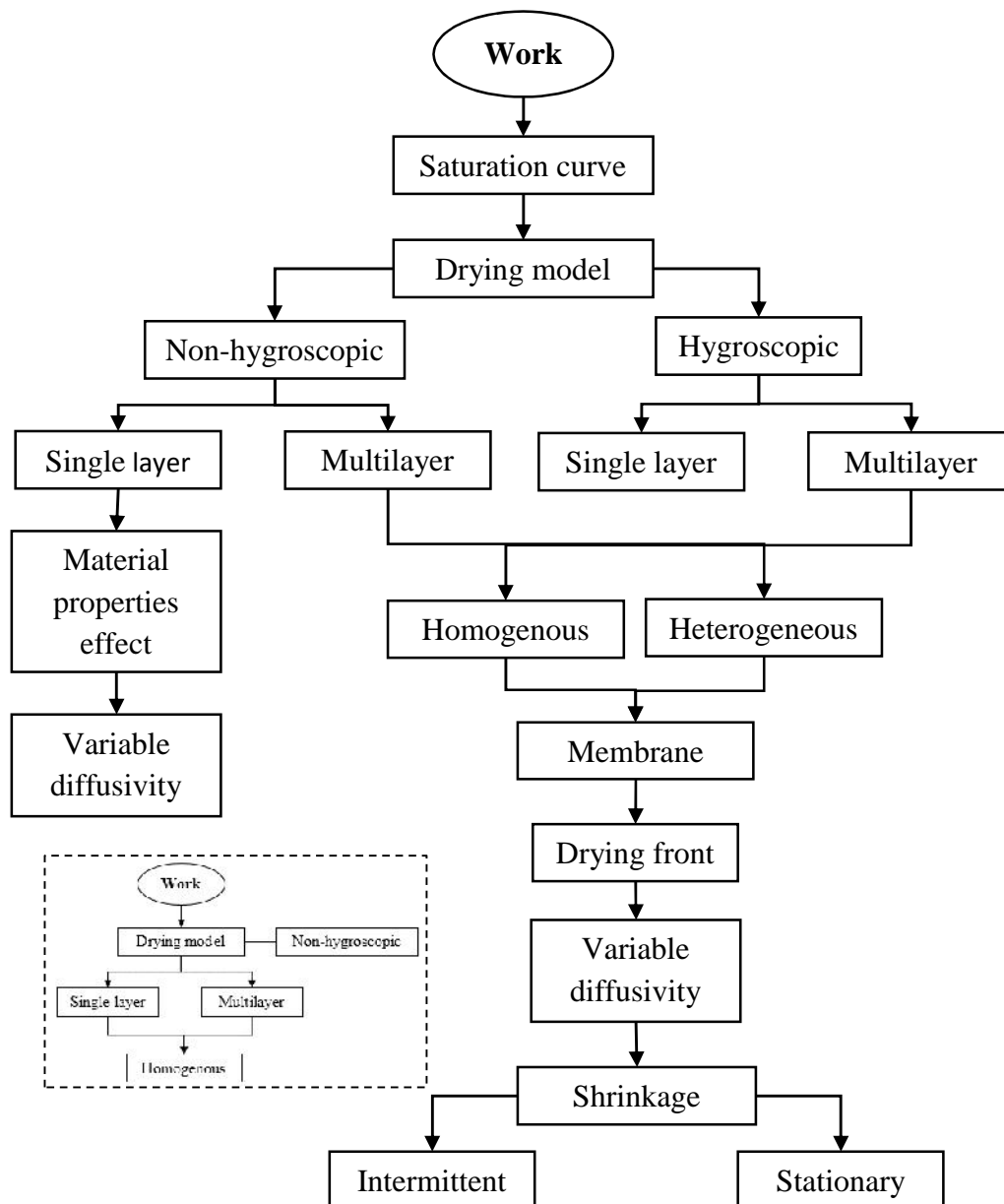


Figure 1.4: Contribution of current work {the insert figure is contribution of previous work}

## 1.6 Structure of the thesis

The research work documented in this thesis is organized to have the following structure: the first chapter consists of a short introduction that includes the problem statement, objectives, scopes and contribution of the current works that have been conducted. The second chapter explains the theory and literature review of the membrane structure, fabrication process of ceramic membrane, the importance of the drying process in the membrane fabrication, drying process theory, transport

properties of porous material and mathematical model of drying. Subsequently, chapter three contains the model governing equations to be derived and incorporated with finite element and numerical solution to solve the nonlinear partial differential equation. Also the background and model set-up for every case study are stated in this chapter. Chapter four includes the validation of the improved proposed model before all the results generated based on different aims for multiple cases will be presented. In every case, the model set-up used and the results, together with the discussion of the results, are presented as independent tasks unless stated otherwise. The major findings of these different cases will be summaries in the final conclusion along with the suggestion of future work to enhance the model (Chapter 5). The Appendices include some additional results.



## **CHAPTER 2**

### **LITERATURE REVIEW**

#### **2.1 Introduction**

Traditionally, ceramic membranes are widely used in wastewater engineering. While ceramic membranes also can be used in any other industries, current trends show they have expanded their application in gas application, chemical industry, biotechnology and the food and beverage industry due to their advantages compared to their competitors, where filtration processes are superior to other separation processes [1]. This is mainly due to ceramic membranes possessing many sterling characteristics as compared to the polymeric membranes, such as much higher chemical and thermal stability. These features enable ceramic membranes to be operated at higher temperatures and in the highly reactive compounds present in either acidic or alkaline surroundings. They also have better physical mechanical stability. Ceramic supported membranes are much harder than the thin polymer structure of the polymeric membranes. Relatively, ceramic membranes will have a longer lifespan compared with polymeric membranes. Overall, these features will save the operation costs for industries without compromising the quality of the products [11]. With those unique characteristics, the efficiency and performance of the filtration system using ceramic membrane also facilitates the membrane structure itself. Thus, understanding the essential features of the membrane structure is crucial for their application and usage in various ranges.

This chapter starts with membrane structure introduction before preparation of ceramic membrane will be discussed. Next, the importance of the drying process is emphasised. Eventually, the drying theory and transport in porous material are discussed, and it ends with various mathematical models.

## 2.2 Membrane structure

In general, a ceramic membrane can be described as a permselective barrier or a fine sieve [1]. The two most important performance indicators for a ceramic membrane is permeability and separation factor. Physical properties such as density, porosity and permeability play an important role when it comes to their applications and separation mechanisms. Typically, ceramic membrane is categorised into four types, namely macroporous, mesoporous, microporous and dense, corresponding to their pore size [1]. Their applications also match with type of ceramic membranes where macroporous and mesoporous ceramic membranes are mainly used in microfiltration (MF) and ultrafiltration (UF) for water treatment industries, while microporous and dense are used in gas separation industries.

Typically, ceramic membranes are often multilayer with one or more different type of ceramic materials. They generally consist of a main microporous (or a dense) top layer, one or two mesoporous intermediate layers and a macroporous support layer. Theoretically, the membrane can be divided into several layers as shown in Figure 2.1 with an illustrated schematic representation in Figure 2.2.

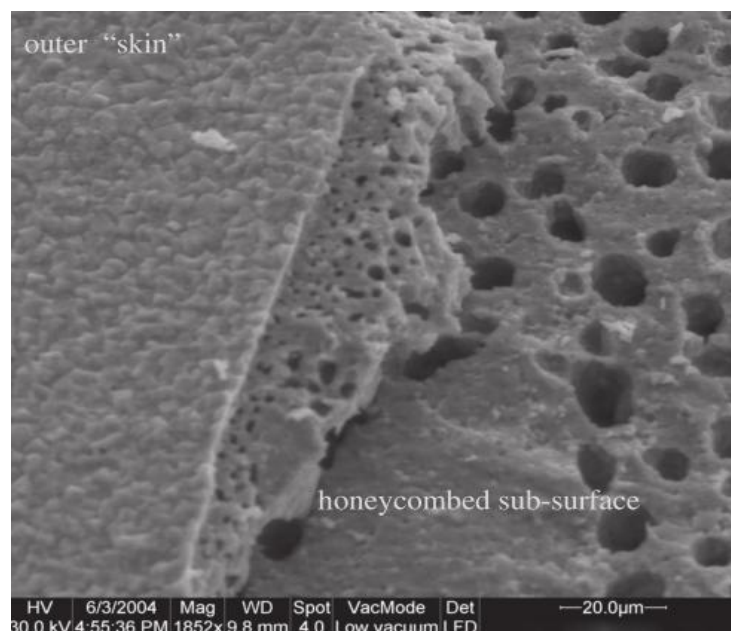


Figure 2.1: SEM micrograph of layered ceramic membrane [1]

The top layer generally has fine and dense pore structure and is used as a filter for separation processes. Meanwhile, the next three layers, which are intermediate and

bottom layer, consist of mesoporous and macroporous ceramic materials respectively, and are fabricated in the form of a porous structure to support the membrane itself and also to ease the permeation process. The pore sizes of the bottom, intermediate and top layers are in the range of  $10\mu\text{m}$ ,  $0.2\text{-}0.7\mu\text{m}$  and  $6\text{nm}$  [1] respectively. Their pore sizes are associated with their aforementioned purpose. The commonly used materials for commercialized ceramic membranes are  $\text{Al}_2\text{O}_3$ ,  $\text{ZrO}_2$ ,  $\text{SiO}_2$ ,  $\text{TiO}_2$  and also a combination of these materials. Obviously, the top separation layer with a microporous and dense ceramic material possesses a hygroscopic property compared to the intermediate and bottom layers that have to be a porous structure and tend to have non-hygroscopic behaviour.

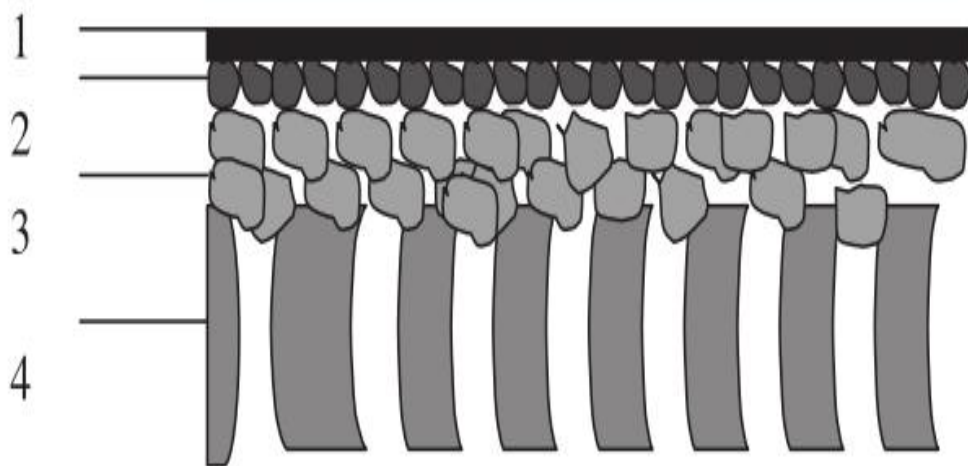


Figure 2.2: Schematic representation of an asymmetric membrane [1]

### 2.3 Preparation of ceramic membrane

Normally, the preparation of ceramic membranes involves three main steps: (1) formation of particle suspensions; (2) packing of the particles in the suspensions into a membrane precursor with a certain shape such as flat sheet, monolith or tube, and (3) consolidation of the membrane precursor by a heat treatment at high temperatures [1]. The generalised flow for ceramic membranes preparation is depicted in Figure 2.3.

The process starts with the determination of the raw materials corresponding with their applications. The materials selection can consist of a single material or a combination of two or more materials for the multilayer membrane structure. Usually the raw materials are in the form of powder. Then the powder formation goes through the spinning and mixing process to form a slurry or paste. There are various methods

for the fabrication of ceramic membranes to form them into the desired shapes depending on their applications and features. Among the common shaping techniques used are slip casting, tape casting, extrusion and pressing, which turn the particle suspension (slurry or paste) into a membrane precursor. The precursor formation then undergoes a drying process which removes water or solvent transports by mass and heat transfer by an evaporation mechanism. Finally, the final membrane product or membrane support can only be obtained through a firing step where the sintering process happens. The sintering process is a consolidation process where denser and better mechanical strength of final product is produced.

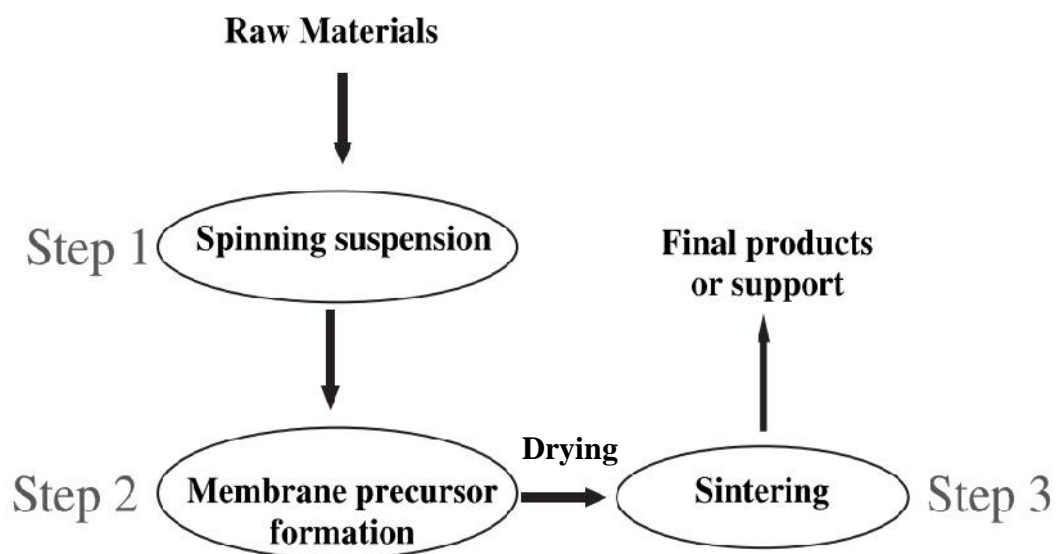


Figure 2.3: Three step procedure for ceramic membranes [1]

The pressing method to form the precursor formation is further discussed as it is often used in related studies. For a fundamental research in the laboratory, this method is widely chosen due to its simplicity in preparation of disc membranes. The dense layer is formed from the particle consolidation by an applied force. This relatively easy press method using a special pressing machine with 100MPa applied pressure has been frequently utilized during the fabrication of oxygen or hydrogen permeable ceramic membranes. The next stage involves drying where moisture is removed from the porous matrix precursor disc. This step is particularly important as massive moisture inside the solid matrix induces great cracking and warping. The sintering process, which is the last stage of consolidation of the disc, leaves the dense product at usually a few cm in diameter and 0.5mm in thickness.

## 2.4 Importance of drying process in ceramic membrane preparation

As one of the most energy intensive processes in industry [4], [22], drying configuration is also the less understood as it involves a lot of variables that change concurrently as the phase and stage changes [23], [24]. Further complications arise if drying involves materials in a multilayer structure [25]. Ceramic membrane layers as aforementioned with a hygroscopic layer involve a bound water mechanism that is strongly attached to the capillary wall. This strongly attached water is quite difficult to measure using experimental techniques due to its strong capillary suction and low permeability value when compared to the non-hygroscopic material [26]. Typically, drying of the membrane layering structure not only involves the controlling of the dynamic parameter or variables but the different materials that act with different properties also strongly influence the consistency of shrinkage geometry which is often associated to leaking of membranes due to the failure of drying and firing processes. Drying induces non-uniform stresses such as pressure gradient of the flow of liquid during shrinkages in constant rate period (CRP), macroscopic pressure gradient of escaping gasses during falling rate period (FRP) and different thermal expansion of ceramic due to temperature gradients, and causes warping or cracking [12]. The flow of liquid, the macroscopic pressure gradient, and the temperature gradient is controlled by the drying rate which is typically controlled by external conditions [12]. A carefully controlled drying process will maintain the desired product configuration [27]. However, insufficient completion of drying and poor condition of the dryer influence directly the product quality [27]. Therefore, an understanding of the various stages and the parameters that evolve dynamically with time throughout the drying process is extremely important in governing the quality of the final products by eliminating all the unnecessary trouble, especially for membrane application. The significance of research and development (R&D) will help to give suggestions and improved design of the product for higher product quality [27]. A precise design for the complete drying process will reduce failures during subsequent sintering to yield a higher quality product.

## 2.5 Drying theory and mechanism of porous structure

To ensure a suitable and usable end product, most of the moisture content must be removed during the drying process [18]. The beginning of the drying of a saturated body is initiated by the free water movement to the air via evaporation mechanism. Meanwhile, an unsaturated body includes the removal of water from a system by first breaking down the strength between the water and the solid surface [28]. Hence, the drying process is such a complex and complicated phenomenon associated with heat and mass transfer within porous media and moisture and is always accompanied by phase changes.

### 2.5.1 Drying period

The individual phase volume using a volume averaging technique usually consists of solid, liquid, bound liquid, gas and water vapour, though each can vary with time and space domain (Figure 2.4). The process that occurs in those phase changes during the drying stages normally includes: unsaturated flow of liquid within the porous solid, vapour flow within the porous solid, liquid vapour phase change, and convective-diffusion transfer of vapour from the surface of the solid to the surroundings [7]. A phase change phenomenon in which the moisture within the material is liquefied or evaporated occurs and there exists two phases simultaneously. Phase changes will divide the solid into wet and dry zones which lead to the latent heat of evaporation existing on the interface.

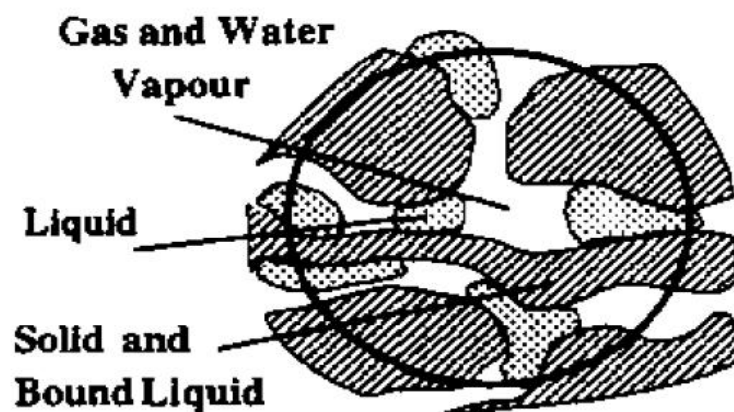


Figure 2.4: Schematic view of phase exists in a porous medium [23]

Those phase changes that occur during the drying of porous media are too complex to describe precisely and thus add difficulties when combined with moisture transport within the matrix. This mechanism can be classified into two distinct stages: stage one is often called the constant drying rate period (CRP) and the second stage known as the falling drying rate period (FRP) is further classified into two different stages (FRP1, FRP2) [29]. The typical drying curve is depicted in Figure 2.5 and this is similarly seen in many works [6], [9], [10], [15], [17], [22], [25], [30]–[36]. As shown in those works involving drying process for ceramic material, the warming up period is non-existent or has no significant effect. Thus this period of drying is not to be included and discussed further in our current works. Hereby, the three distinguishable stages namely CRP, FRP1 and FRP2 that highly influence and contribute as a decisive factor in the heat and mass transfer through the drying process are further elaborated.

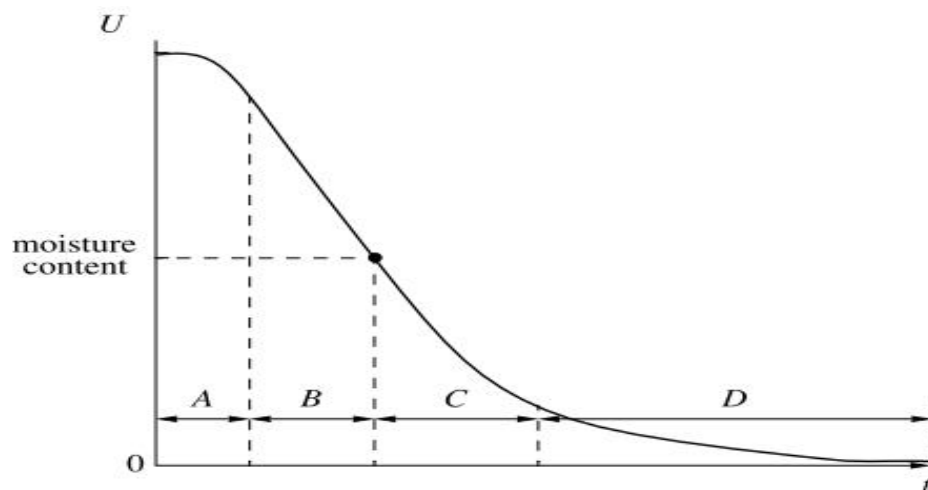


Figure 2.5: A typical moisture content profile. (A) Warm-up period. (B) Constant rate period. (C) First falling rate period. (D) Second falling rate period. [37]

The first stage of the drying process, called the CRP, attributes to the constant drying rate as the rate of evaporation per unit area of the drying surface is independent of time [9]. Drying at this stage can be presumed to be free evaporation from an open dish of liquid. Initial moisture content and hydraulic diffusivity of porous materials are sufficiently high enough and the entire surface area is covered with a film of free water [6], [22]. This leads to liquid continuously evaporating without being replaced by air where the area of contact between the air and the medium is constant. The mass flux (mass loss per unit of time and area) is constant in this state. The evaporation rate is

maintained mainly by adequate capillary force associated with other forces such as liquid-solid matrix interfacial drag, viscous force and others [10]. Liquid migrates from regions of high concentration of moisture content in large pores towards the low concentration of moisture content in the small pores. This liquid migration is associated with Darcy's law [23], [26], [38]. During CRP, the water distribution does not show steep internal gradients [8] because the internal moisture transfer to the surface and the evaporation from the surface are in equilibrium. This stage of drying is also referred to as a funicular state. The temperature of the solid matrix remains at wet bulb temperature because no energy transfer occurs [39]. The convective heat supply to the interface is quasi entirely used for the evaporation of water. Thus, the drying rate is greatest at CRP and depends only on the external conditions such as temperature, relative humidity, velocity and others, rather than the rate of transport within the material itself [8], [10], [23].

As drying proceeds, the surface water content falls rapidly while the fraction of wet area at the surface also decreases. Eventually, the drying process reaches the critical moisture content denoting the point on the drying curve at which the transition from the CRP to the FRP takes place [17]. The corresponding free water level holds the saturation value of 0.3 for most porous materials [10], [20], [40]. This is the second stage of the drying process (FRP). Further, FRP can be separated into two distinct periods, denoted as falling rate period one (FRP1) and falling rate period two (FRP2). FRP1 happens once insufficient free water passes through randomly distributed paths in a medium leading to a formation of the percolation threshold. Consequently, the water phase will continue when the free water content is above the critical value, and the formation of discontinuous wet patches on the surface occurs once the free water level is below critical regardless of the rate of internal moisture transfer. Those dry patches formed on the surface will still contain bound water in their pores and it offers a resistance to heat transport, resulting in a reduction of evaporation rate as well as drying rate. This phenomenon will cause the formation of a drying front, marked by a steep change in liquid-vapour content [22], [41]. At this moment, the external vapour flux is reduced and heat flux from the surroundings being supplied to the solid matrix is greater than what is needed for evaporation to occur. Eventually, the temperature at the surface will increase. This is followed by the inner part of the solid as a conductive heat flux will exist inside it, increasing the temperature within the solid to enable evaporation to continue by gaseous diffusion. It is also likely that steeper gradients of



water will develop behind the drying surface following the increase of surface temperature initially [8]. At this moment, a capillary mechanism which is dominated before FRP1 slowly diminishes as the water is strongly bonded to the porous matrix. Vapour movement by diffusion will control the much slower drying rate at this moment associated with the decrease in moisture content. Vapour flows from many vapour molecular regions to the low vapour molecular regions and the vapour diffusion is associated with Fick's law [18], [26]. Finally, the drying process eventually ceases when the moisture content reaches equilibrium, denoting the final value at the end of drying [17]. The end of this drying process at this stage is generally only applicable for non-hygroscopic material. As for hygroscopic material which exhibits a bound water mechanism, the drying will proceed to the next stage.

Further drying leads to surface water content reaching the maximum irreducible value and there is no free water on the surface. Dry patches appear followed by an increase of surface temperature signalling the start of FRP2. The formation of an evaporation front divides the solid into two regions as shown in Figure 2.6. Inside the evaporation front, there is free water existing in the pores and a capillary mechanism plays a role in transporting the liquid for evaporation to happen. Outside the evaporation front, there is no free water and all water will be bound to the solid matrix [10], [28]. The pendular state follows the funicular state where only bound water exists. The drying of bound water only occurs in hygroscopic materials and its mechanism is discussed in the later sub-section.

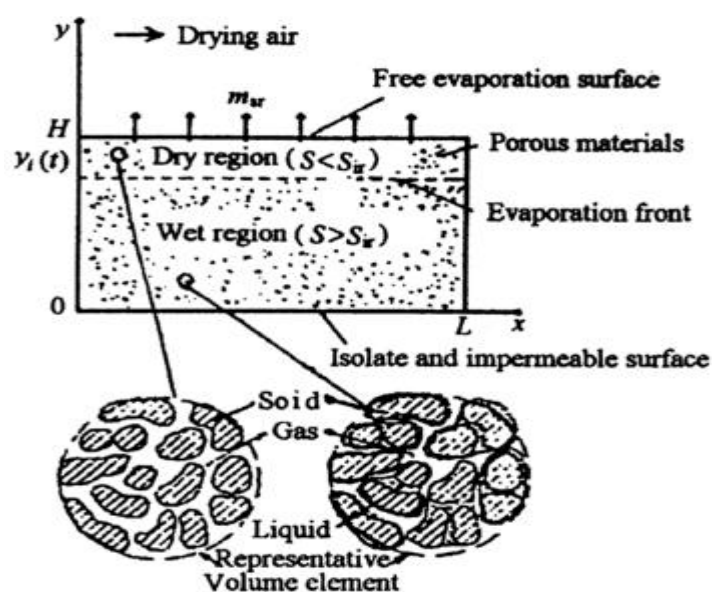


Figure 2.6: Drying model [10]

### 2.5.2 Kinetic of dynamic drying diffusivity

There are various drying parameters that evolve concurrently during mass and heat transfer. Among the common main variables are water pressure, temperature, gas pressure and moisture content. The expression of variables changes corresponding to the related effective diffusivity in the model. Hence, the expression of the diffusivity in the model determines its validity. The effective diffusivity is not assumed to be constant but to be functional of temperature or moisture content [26], [42]. Since the effective diffusivity depends on the heat and mass transfer mechanisms considered, it is important to analyse these transport phenomena to develop a robust model for practical application. The variations of effective diffusivity are shown in Figure 2.7. As illustrated, the different mechanism of the effective diffusivity depends critically on the saturation condition. When the saturation is above the critical value, liquid movement is dominantly generated by capillary action. The concept of capillary action will be discussed in the later sub-section. This is noted by the high value of the liquid diffusivity when saturation is high, and it reduces sharply when saturation nears the critical stage. A substitution for capillary action is the vapour mechanism for mass transfer mainly due to diffusion. This is shown by the obvious increment of vapour diffusivity as evaporation continues. Towards the end of the drying process, the vapour diffusion decreases gradually as the moisture equilibrium between the solid matrix and external surroundings is almost accomplished. It can be deduced that the total diffusivity is the combination of these effective diffusivity stages during the drying processes. The stages of drying can also be interpreted with this data. Unfortunately, the effective diffusivity is non-empirical data and largely unavailable or almost non-existent for most materials [26]. Therefore, a mathematical drying model needs to be developed for the purpose of improving knowledge of the interrelationship of effective diffusivity for a particular material structure.

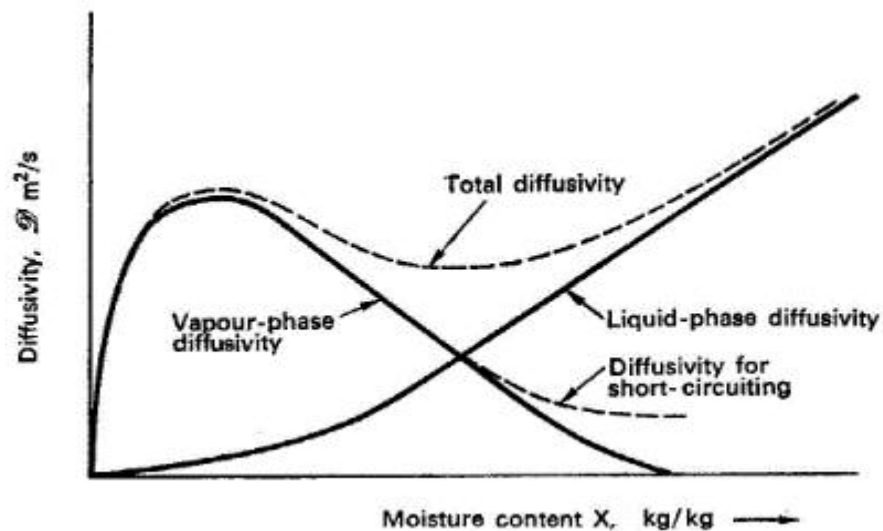


Figure 2.7: Variations of effective diffusivity with moisture content [43]

### 2.5.3 Drying in non-hygroscopic and hygroscopic materials

Generally, moisture in a porous material consists of three types of water identified as free, capillary, and bound water. Free water is able to flow under an applied pressure gradient, capillary water is immobile water held by capillary forces in regions of microporosity i.e. dead-end pores, while bound water includes both the water strongly held to negatively charged particle surfaces and the water of hydration associated with the mineral charge-balancing unit. The difference level of these types of water will exhibit different properties of porous material generally known as hygroscopic and non-hygroscopic materials. The drying of non-hygroscopic materials only involves free and capillary water that can easily be determined and measured with specific equipment. In contrast, the drying of hygroscopic materials not only involves free and capillary water but also tightly bound water that is strongly attached to the solid matrix up to the hydration temperature [44]. By referring to Figure 2.5, the drying period for non-hygroscopic material consists of periods A, B and C but for hygroscopic material, it is further extended until period D before the drying ceases. Previous studies on drying of hygroscopic and non-hygroscopic materials have presented different equations and formulations as well as the concept that has been derived [10], [40], [45], [46]. Bound water movement is expressed in terms of the diffusion of sorbed water driven by a gradient in the chemical potential of the sorbed water molecules [45]. A similar approach had been used by Kolhapure [44] during studies of an unsaturated flow of low moisture for porous hygroscopic material. As for Stanish et

al. [46], in low moisture contents, pores mainly consist of bound water and vapour in their development and had derived a uniquely explicit expression for bound-water flux in terms of temperature and vapour pressure gradients. Meanwhile, Zhang et al. [10] and Haghi [37] revealed that the bound water transport mechanism is only effective when saturation irreducible is reached. The movement of bound water in hygroscopic materials is also known as liquid moisture transfer near dryness or sorption diffusion with a driving force of vapour transport and without liquid transport [5]. Thus, the drying of different types of moisture content is associated with the material behaviour and the drying stage.

#### 2.5.4 Drying shrinkage

Water on a porous matrix exists with a potential for occupying pores. The gradient of suction potential in clay material corresponding to moisture content is identified as the driving force for water movement inside the porous matrix [47]. The suction potential and strain induced are interrelated and cannot be discussed without taking both into account in the shrinkage problem [20], [27], [30], [32], [47], [48]. A detailed description of the shrinkage phenomenon is of vital importance to study as improper control of drying-induced stresses lead to the permanent irreversible deformation of dried products which causes destruction and defects such as warping, cracking and fracture [6], [27], [32], [49]–[52]. In general, material undergoing drying induced several types of strain and in many cases, the largest strain component is the shrinkage strain [23]. Theoretically, material shrinkage can be ascertained by considering the body volume or any geometry changes caused by reduction of moisture gradient or state of saturation [17], [29], [53]–[55]. As reported in many open literatures, a linear shrinkage correlation with moisture content is shown [17], [23], [27], [32], [56]. The typical equation that has widely been used is:

$$\frac{V_t}{V_0} = s_1 + s_2 S \quad (2.1)$$

where  $V_t$  and  $V_0$  denote the final volume and initial volume respectively,  $S$  is the saturation and  $s_1$  and  $s_2$  are the constants. The relationship between drying rate,

moisture content and volume shrinkage is shown in Figure 2.8. The greatest shrinkage happens during the CRP [6], [27], [29], [47], [56]–[59]. During CRP, the outflow of liquid-water is induced by a high gradient of pore water pressure between the surface and core of the matrix. Thus, the continuous liquid supply from the capillary mechanism via water flux is constant depending on the external drying condition [55]. The fully saturated wet state of material dried is expanding shrinkage at the maximum limits [12]. Therefore, effective stress increases due to a decrease in the water pressure and the matrix suffers an increasing internal compression state of stress. Therefore, the particles inside the solid matrix have to rearrange and shrink [6], [12], [41]. However, the dried product is free of stress at this moment [49] if there is no crack formation being observed in this period [30] (refer Figure 2.9(a)). The critical point of saturation is also the crack initiation point [32]. There is much lower shrinkage in FRP but it tends to generate fracture failure increase as the dried body is exposed to very intensive shrinkage before that. At this moment, the particles are in close contact or are touching each other. This leads to minimal or no shrinkage beyond this period of drying. This is called the shrinkage limit [48], [60], [61]. Commonly, the formation crack is initialised when an evaporation front or receding drying reaches the surface layer gradually at FRP. The formation of water-air meniscus between the particles also leads to capillary suction between the particles (refer Figure 2.9(b)). Over a prolonged period of time, the suction between particles increases due to a decrease in moisture content. When the layer consolidates and shrinks, tensile stress is formed at the surface layer (refer to Figure 2.9(c)). Hereby, the generation of tensile stress counteracts the shrinkage phenomenon. When wet material dries, the drier surface intensively shrinks but is restrained by the wet core. Hence, the surface is in a tensional state of stress while the core is in a compressional one [19], [20], [29], [55], [56], [59]. When the rising tensile stress exceeds the tensile strength of the surface layer, a cracking formation occurs on the surface (refer to Figure 2.9(d)) caused by inhomogeneous shrinkage when the rigid outer region restrains the inner saturated regions to shrink [6], [19], [20], [30], [41], [49], [56]. Often, a number of internal small micro cracks arise during drying. This is a local weakness of the material which may nucleate and develop into bigger macro cracks that have potential to create failure or fracture at any time [19], [49], [56]. Furthermore, the confirmation of dry drained zones formation at different extension and orientation with respect to the stress field increases the probability of crack initiation [41].

## REFERENCES

- [1] K. Li, *Ceramic Membranes for Separation and Reaction*, vol. 59, no. 3. Chichester: John Wiley & Sons Ltd, 2007.
- [2] R. Hill, "Industry Report Membranes," San Diego, 2011.
- [3] M. N. Rahaman, *Ceramic Processing*. Boca Raton: Taylor & Francis Group, 2007.
- [4] A. S. Mujumdar, Ed., *Handbook of Industrial Drying*, Third. Boca Raton, USA: Taylor & Francis Group, 2006.
- [5] T. Defraeye, B. Blocken, and D. Derome, "Convective heat and mass transfer modelling at air-porous material interfaces: overview of existing methods and relevance," *Chem. Eng. Sci.*, vol. 74, pp. 49–58, 2012.
- [6] A. Tarantino, A. Sacchet, R. Dal Maschio, and F. Francescon, "A Hydromechanical Approach to Model Shrinkage of Air-Dried Green Bodies," *J. Am. Ceram. Soc.*, vol. 93, no. 3, pp. 662–670, 2010.
- [7] C. Hall, W. Hoff, and M. Nixon, "Water movement in porous building materials—VI. Evaporation and drying in brick and block materials," *Build. Environ.*, vol. 19, no. 1, pp. 13–20, 1984.
- [8] C. Hall and W. Hoff, *Water transport in brick, stone and concrete*, Second. London and New York: CRC Press, 2012.
- [9] G. Scherer, "Theory of Drying," *J. Am. Ceram. Soc.*, vol. 73, no. 1, pp. 3–14, 1990.

- [10] Z. Zhang, S. Yang, and D. Liu, "Mechanism and mathematical model of heat and mass transfer during convective drying of porous materials," *Heat Transf.-Asian Res.*, vol. 28, no. 5, pp. 337–351, 1999.
- [11] W. D. Callister and D. G. Rethwisch, *Materials Science and Engineering*, Eighth. USA: John Wiley & Sons, Inc, 2011.
- [12] T. A. Ring, "Green Body Drying," in *Fundamentals of Ceramic Powder Processing and Synthesis*, San Diego: Academic Press, 1996, pp. 683–728.
- [13] F. H. Norton, "Clay - Why It Acts the Way It Does," *Studio Potter 4*, 1976.
- [14] T. Defraeye, "Advanced computational modelling for drying processes – A review," *Appl. Energy*, vol. 131, pp. 323–344, 2014.
- [15] R. B. Keey, *Drying Principals and Practice*. Oxford: Pergamon Press, 1972.
- [16] S. J. Kowalski and A. Pawłowski, "Intermittent drying of initially saturated porous materials," *Chem. Eng. Sci.*, vol. 66, no. 9, pp. 1893–1905, 2011.
- [17] S. J. Kowalski and D. Mierzwa, "Numerical analysis of drying kinetics for shrinkable products such as fruits and vegetables," *J. Food Eng.*, vol. 114, no. 4, pp. 522–529, 2013.
- [18] I. Turner, J. Puiggali, and W. Jomaa, "A numerical investigation of combined microwave and convective drying of a hygroscopic porous material: A study based on pine wood," *Chem. Eng. Res. Des.*, vol. 76, no. Part A, pp. 193–209, 1998.
- [19] J. Banaszak and S. J. Kowalski, "Theoretical and experimental analysis of stresses and fractures in clay like materials during drying," *Chem. Eng. Process. Process Intensif.*, vol. 44, no. 4, pp. 497–503, Apr. 2005.
- [20] S. J. Kowalski, K. Rajewska, and A. Rybicki, "Destruction of wet materials by drying," *Chem. Eng. Sci.*, vol. 55, pp. 5755–5762, 2000.

- [21] F. Kallel, N. Galanis, B. Perrin, and R. Javelas, "Effects of moisture on temperature during drying of consolidated porous materials," *J. Heat Transfer*, vol. 115, pp. 724–733, 1993.
- [22] N. Shahidzadeh-Bonn, A. Azouni, and P. Coussot, "Effect of wetting properties on the kinetics of drying of porous media," *J. Phys. Condens. Matter*, vol. 19, no. 11, p. 112101, 2007.
- [23] P. Perré, R. Remond, and I. Turner, "Comprehensive drying models based on Volume Averaging: Background, Application and Perspective," in *Modern Drying Technology*, Volume 1., E. Tsotsas and A. S. Mujumdar, Eds. Weinheim: Wiley VCH Verlag GmbH & Co. KGaA, 2007, pp. 1–12.
- [24] P. Rattanadecho, W. Pakdee, and J. Stakulcharoen, "Analysis of multiphase flow and heat transfer: Pressure buildup in an unsaturated porous slab exposed to hot gas," *Dry. Technol.*, vol. 26, pp. 39–53, 2007.
- [25] Z. Harun and D. T. Gethin, "Drying Simulation of Ceramic Shell Build Up Process," *2008 Second Asia Int. Conf. Model. Simul. AMS*, pp. 794–799, 2008.
- [26] A. K. Datta, "Porous media approaches to studying simultaneous heat and mass transfer in food processes. I: Problem formulations," *J. Food Eng.*, vol. 80, no. 1, pp. 80–95, May 2007.
- [27] Z. X. Gong, A. S. Mujumdar, Y. Itaya, S. Mori, and M. Hasatani, "Drying of Clay and Nonclay Media : Heat and Mass Transfer and Quality Aspects," *Dry. Technol.*, vol. 16, no. 6, pp. 1119–1152, Jan. 1998.
- [28] D. J. Lee, A. Su, and A. S. Mujumdar, "Bound Water Content in Wet Materials," *Dry. Technol.*, vol. 31, no. 2, pp. 202–206, Jan. 2013.
- [29] S. J. Kowalski, "Thermomechanical Approach To Shrinking and Cracking Phenomena in Drying," *Dry. Technol.*, vol. 19, no. 5, pp. 731–765, May 2001.
- [30] H. Colina and S. Roux, "Experimental model of cracking induced by drying shrinkage," *Eur. Phys. J. E*, vol. 194, pp. 189–194, 2000.



- [31] Z. Harun and D. T. Gethin, "Drying(consolidation) porous ceramic by considering the microscopic pore temperature gradient," *Appl. Mech. Mater.*, vol. 147, pp. 210–214, 2012.
- [32] J. Nascimento, A. Lima, and E. Santana, "Experimental drying of ceramic bricks including shrinkage," in *18th International Congress of Mechanical Engineering*, 2005, pp. 1–7.
- [33] K. Murugesan, H. R. Thomas, and P. J. Cleall, "An investigation of the influence of two-stage drying conditions on convective drying of porous materials," *Int. J. Numer. Methods Heat Fluid Flow*, vol. 12, no. 1, pp. 29–46, Feb. 2002.
- [34] H. Suresh and K. Murugesan, "Drying of Porous Material Using Finite Element Method," in *Second International Conference on CFD in the Minerals and Process Industries*, 1999, no. December, pp. 163–168.
- [35] R. Prommas, "Theoretical and experimental study of heat and mass transfer mechanism during convective drying of multi-layered porous packed bed," *Int. Commun. Heat Mass Transf.*, vol. 38, no. 7, pp. 900–905, Aug. 2011.
- [36] J. Van Brakel, "Mass transfer in convective drying," *Adv. Dry.*, vol. 1, pp. 217–267, 1980.
- [37] A. K. Haghi, "Transport phenomena in porous media: A review," *Theor. Found. Chem. Eng.*, vol. 40, no. 1, pp. 14–26, Jan. 2006.
- [38] T. Kanno, K. Kato, and J. Yamagata, "Moisture movement under a temperature gradient in highly compacted bentonite," *Eng. Geol.*, vol. 41, no. 1–4, pp. 287–300, Jan. 1996.
- [39] S. J. Kowalski and K. Rajewska, "Drying-induced stresses in elastic and viscoelastic saturated materials," *Chem. Eng. Sci.*, vol. 57, no. 18, pp. 3883–3892, Sep. 2002.
- [40] A. K. Haghi, "Thermal Analysis of Drying Process: A theoretical approach," *J. Therm. Anal. Calorim.*, vol. 74, pp. 827–842, 2003.

- [41] H. Peron, T. Hueckel, L. Laloui, and L. B. Hu, "Fundamentals of desiccation cracking of fine-grained soils: experimental characterisation and mechanisms identification," *Can. Geotech. J.*, vol. 46, no. 10, pp. 1177–1201, Oct. 2009.
- [42] Z. H. Wang and G. Chen, "Heat and mass transfer during low intensity convection drying," *Chem. Eng. Sci.*, vol. 54, no. 17, pp. 3899–3908, Sep. 1999.
- [43] J. R. Philip and D. A. De Vries, "Simultaneous Transfer of Heat and Moisture in Porous Media," *Trans. Am Geophys Union*, vol. 39, pp. 909–916, 1958.
- [44] N. Kolhapure and K. Venkatesh, "An unsaturated flow of moisture in porous hygroscopic media at low moisture contents," *Chem. Eng. Sci.*, vol. 52, no. 19, pp. 3383–3392, 1997.
- [45] J. F. Siau and Z. Jin, "Nonisothermal moisture diffusion experiments analyzed by four alternative equations," *Wood Sci. Technol.*, vol. 19, pp. 151–157, 1985.
- [46] M. A. Stanish, G. S. Schajer, and F. Kayihan, "A mathematical model of drying for hygroscopic porous media," *AIChE J.*, vol. 32, no. 8, pp. 1301–1311, Aug. 1986.
- [47] Y. Itaya, S. Mori, and M. Hasatani, "Drying of Ceramics," in *Handbook of Industrial Drying*, 3rd ed., A. S. Mujumdar, Ed. Boca Raton: CRC Press, 1992, pp. 729–741.
- [48] F. Augier, W. J. Coumans, A. Hugget, and E. F. Kaasschieter, "On the risk of cracking in clay drying," *Chem. Eng. J.*, vol. 86, pp. 133–138, 2002.
- [49] S. J. Kowalski, "Control of mechanical processes in drying. Theory and experiment," *Chem. Eng. Sci.*, vol. 65, no. 2, pp. 890–899, Jan. 2010.
- [50] A. B. Cerato and A. J. Lutenegger, "Shrinkage of Clays," in *Proceedings of the Fourth International Conference on Unsaturated Soils*, 2006, no. 405, pp. 1097–1108.

- [51] A. A. J. Ketelaars, E. F. Kaasschieter, W. J. Coumans, and P. J. A. M. Kerkhof, "The influence of shrinkage on drying behaviour of clays," *Dry. Technol.*, vol. 12, no. 7, pp. 1561–1574, 1994.
- [52] G. Musielak, "Possibility of clay damage during drying," *Dry. Technol.*, vol. 19, no. 8, pp. 1645–1659, 2001.
- [53] A. Wysocka, W. Stepniewski, and R. Horn, "Shrinkage properties of three clay materials at different temperatures," *Int. Agrophysics*, vol. 20, no. 2006, pp. 255–260, 2006.
- [54] M. S. Belopol'skii, "Determining the plasticity of clays and ceramic bodies," *Glas. Ceram.*, vol. 34, no. 5, pp. 306–307, May 1977.
- [55] F. Pourcel, W. Jomaa, J.-R. Puiggali, and L. Rouleau, "Criterion for crack initiation during drying: Alumina porous ceramic strength improvement," *Powder Technol.*, vol. 172, no. 2, pp. 120–127, Mar. 2007.
- [56] G. Musielak and T. Liwa, "Fracturing of Clay During Drying: Modelling and Numerical Simulation," *Transp. Porous Media*, vol. 95, no. 2, pp. 465–481, Aug. 2012.
- [57] Y. Itaya, S. Mori, and M. Hasatani, "Effect of Intermittent Heating on Drying-Induced Strain-Stress of Molded Clay," *Dry. Technol.*, vol. 17, no. 7–8, pp. 1261–1271, Aug. 1999.
- [58] Y. Itaya, K. Okouchi, and S. Mori, "Effect of Heating Modes on Internal Strain–Stress Formation During Drying of Molded Ceramics," *Dry. Technol.*, vol. 19, no. 7, pp. 1491–1504, Jul. 2001.
- [59] S. J. Kowalski, G. Musielak, and a. Rybicki, "The response of dried materials to drying conditions," *Int. J. Heat Mass Transf.*, vol. 40, no. 5, pp. 1217–1226, Mar. 1997.
- [60] S. Chakrabarti, J. Sahu, A. Biswas, and H. N. Acharya, "Relationship between weight loss and shrinkage during gel drying," *J. Mater. Sci. Lett.*, vol. 11, no. 11, pp. 763–766, 1992.

- [61] H. Krisdani, H. Rahardjo, and E.-C. Leong, "Effects of different drying rates on shrinkage characteristics of a residual soil and soil mixtures," *Eng. Geol.*, vol. 102, no. 1–2, pp. 31–37, Nov. 2008.
- [62] W. D. Kingery, *Introduction to Ceramics*, 1st ed. Wiley-Interscience, 1960.
- [63] C. Tang, B. Shi, C. Liu, W. Suo, and L. Gao, "Applied Clay Science Experimental characterization of shrinkage and desiccation cracking in thin clay layer," *Appl. Clay Sci.*, vol. 52, no. 1–2, pp. 69–77, 2011.
- [64] N. Yesiller, C. J. Miller, G. Inci, and K. Yaldo, "Desiccation and cracking behavior of three compacted landfill liner soils," vol. 57, pp. 105–121, 2000.
- [65] S. J. Kowalski and A. Pawłowski, "Drying of Wet Materials in Intermittent Conditions," *Dry. Technol.*, vol. 28, no. 5, pp. 636–643, May 2010.
- [66] S. J. Kowalski and A. Pawłowski, "Energy consumption and quality aspect by intermittent drying," *Chem. Eng. Process. Process Intensif.*, vol. 50, no. 4, pp. 384–390, Apr. 2011.
- [67] C. Kumar, M. A. Karim, and M. U. H. Joardder, "Intermittent drying of food products: A critical review," *J. Food Eng.*, vol. 121, pp. 48–57, Jan. 2014.
- [68] B. A. Manel, D. Mihoubi, S. Jalila, and B. Ahmed, "Strain – Stress Formation During Stationary and Intermittent Drying of Deformable Media," *Dry. Technol.*, vol. 32, pp. 1245–1255, 2014.
- [69] S. J. Kowalski and A. Pawłowski, "Modeling of Kinetics in Stationary and Intermittent Drying," *Dry. Technol.*, vol. 28, no. 8, pp. 1023–1031, Jul. 2010.
- [70] D. G. Fredlund and A. Xing, "Equations for the soil-water characteristic curve," *Can. Geotech. J.*, vol. 31, no. 3, pp. 521–532, 1994.
- [71] A. Stevenson, Ed., *Oxford Dictionary of English*, 3rd Revise. Oxford, USA: Oxford University Press, 2010.

- [72] A. K. Datta, "Porous media approaches to studying simultaneous heat and mass transfer in food processes. II: Property data and representative results," *J. Food Eng.*, vol. 80, no. 1, pp. 96–110, May 2007.
- [73] A. O. Shepard, *Ceramics for the Archaeologist*, vol. 23, no. 1. Washington: Carnegie Institution Publication 609, 1957.
- [74] S. Whitaker, "Simultaneous Heat, Mass, and Momentum Transfer in Porous Media: A Theory of Drying," *Adv. heat Transf.*, vol. 13, pp. 119–203, 1977.
- [75] S. Witharana, C. Hodges, D. Xu, X. Lai, and Y. Ding, "Aggregation and settling in aqueous polydisperse alumina nanoparticle suspensions," *J. Nanoparticle Res.*, vol. 14, no. 5, p. 851, Apr. 2012.
- [76] A V Schmitz, Y. S. Mutlu, E. Glatt, S. Klein, and B. Nestler, "Flow simulation through porous ceramics used as a throttle in an implantable infusion pump.," *Biomed. Tech. (Berl.)*, vol. 57, no. Suppl 1, pp. 277–280, Jan. 2012.
- [77] Y. R. Mayhew and G. G. C. Rogers, *Thermodynamic and Transport Properties of Fluids*. Oxford: Blackwell, 1976.
- [78] I. Ioannou, C. Hall, M. A. Wilson, W. D. Hoff, and M. A. Carter, "Direct measurement of the wetting front capillary pressure in a clay brick ceramic," *J. Phys. D. Appl. Phys.*, vol. 36, no. 24, pp. 3176–3182, Dec. 2003.
- [79] M. Tuller and D. Or, *Water retention and characteristic curve*, Volume 4. Oxford, U. K: Elsevier, 2004.
- [80] Y. Mualem, "A new model for predicting the hydraulic conductivity of unsaturated porous media," *Water Resour. Res.*, vol. 12, no. 3, pp. 513–522, 1976.
- [81] M. Tuller and D. Or, "Water retention and characteristic curve," in *Encyclopedia of Soils in the Environment*, Volume 4., Oxford: Elsevier Ltd., 2005, pp. 278–289.

- [82] R. H. Brooks and A. T. Corey, "Hydraulic properties of porous media," Colorado State University, Fort Collins, Colorado, 1964.
- [83] M. Van Genuchten, "A closed-form equation for predicting the hydraulic conductivity of unsaturated soils," *Soil Sci. Soc. Am. J.*, vol. 8, pp. 892–898, 1980.
- [84] Y. Wang, S. M. Grove, and M. G. Anderson, "A physical–chemical model for the static water retention characteristic of unsaturated porous media," *Adv. Water Resour.*, vol. 31, no. 4, pp. 701–713, Apr. 2008.
- [85] J. Touma, "Comparison of the soil hydraulic conductivity predicted from its water retention expressed by the equation of Van Genuchten and different capillary models," *Eur. J. Soil Sci.*, vol. 60, no. 4, pp. 671–680, Aug. 2009.
- [86] M. G. Hodnett and J. Tomasella, "Marked differences between van Genuchten soil water-retention parameters for temperate and tropical soils: a new water-retention pedo-transfer functions developed for tropical soils," *Geoderma*, vol. 108, no. 3–4, pp. 155–180, Aug. 2002.
- [87] B. Lin and A. B. Cerato, "Hysteretic soil water characteristics and cyclic swell–shrink paths of compacted expansive soils," *Bull. Eng. Geol. Environ.*, vol. 72, no. 1, pp. 61–70, Jan. 2013.
- [88] K.C. Ma, Y.C. Tan, and C.H. Chen, "The influence of water retention curve hysteresis on the stability of unsaturated soil slopes," *Hydrol. Process.*, vol. 25, no. 23, pp. 3563–3574, Nov. 2011.
- [89] L. Wang, Z. Li, W. ke Wang, and Y. T. Li, "Measurement of soil moisture characteristic curves of sandy medium by sandy funnel method," in *ISWREP 2011 - Proceedings of 2011 International Symposium on Water Resource and Environmental Protection*, 2011, vol. 3, pp. 1885–1887.
- [90] V. Baroghel-Bouny, M. Mainguy, T. Lassabatere, and O. Coussy, "Characterization and identification of equilibrium and transfer moisture

- properties for ordinary and high-performance cementitious materials,” *Cem. Concr. Res.*, vol. 29, no. 8, pp. 1225–1238, Aug. 1999.
- [91] J. R. Philip and D. A. De Vries, “Moisture movement in porous materials under temperature gradients,” *Eos, Trans. Am. Geophys. Union*, vol. 38, pp. 222–232, 1957.
- [92] E. Romero, A. Gens, and A. Lloret, “Temperature effects on the hydraulic behaviour of an unsaturated clay,” *Geotech. Geol. Eng.*, vol. 19, pp. 311–332, 2001.
- [93] S. A. Grant and A. Salehzadeh, “Calculations of the temperature effects on wetting coefficients of the porous solids and their capillary pressure functions,” *Water Resour. Reseach*, vol. 32, pp. 261–279, 1996.
- [94] Z. Harun, “Simulation of drying for multilayer investment casting shells,” Swansea University, 2007.
- [95] H. C. Huang and A. S Usmani, *Finite Element Analysis for Heat Transfer*, 1st ed. London: Springer-Verlag, 1994.
- [96] T. Sherwood, “The drying of solids,” *Ind Engng Chem*, no. 21, pp. 12–16, 1929.
- [97] A. V Luikov, “Systems of differential equations of heat and mass transfer in capillary-porous bodies (review),” *Int. J. Heat Mass Transf.*, vol. 18, no. 1, pp. 1–14, Jan. 1975.
- [98] P. Horacek, “Modeling of Coupled Moisture and Heat Transfer During Wood Drying,” in *8th International IUFRO Wood Drying Conference*, 2003, pp. 372–378.
- [99] L. Pel, K. Kopinga, and H. Brocken, “Moisture transport in porous building materials,” *Heron*, vol. 41, no. 2, pp. 95–105, 1996.
- [100] K. Murugesan, H. . Suresh, K. . Seetharamu, P. . Aswatha Narayana, and T. Sundararajan, “A theoretical model of brick drying as a conjugate problem,” *Int. J. Heat Mass Transf.*, vol. 44, no. 21, pp. 4075–4086, Nov. 2001.

- [101] A. Derossi, C. Severini, and D. Cassi, *Mass Transfer Mechanisms during Dehydration of Vegetable Food: Traditional and Innovative Approaches, Advanced Topics in Mass Transfer*. 2011.
- [102] D. Or, P. Lehmann, and N. Shokri, “Characteristic lengths affecting evaporation from heterogeneous porous media with sharp textural boundaries,” *Estud. la Zo. No Saturada del Suelo*, vol. VIII, pp. 1–8, 2007.
- [103] S. J. Kowalski and A. Rybicki, “The vapour–liquid interface and stresses in dried bodies,” *Transp. porous media*, vol. 66, pp. 43–58, 2007.
- [104] H. R. Thomas and W. J. Ferguson, “A fully coupled heat and mass transfer model incorporating contaminant gas transfer in an unsaturated porous medium,” *Comput. Geotech.*, vol. 24, no. 1, pp. 65–87, Jan. 1999.
- [105] J. R. Philip and D. A. De Vries, “The Theory of Heat and Moisture Transfer in Porous Media Revisited,” *Int. J. Heat Mass Transf.*, vol. 30, pp. 1343–1350, 1987.
- [106] N. E. Edlefsen and A. B. C. Anderson, “Thermodynamics of soil moisture,” *Hilgardia*, vol. 15, pp. 31–298, 1943.
- [107] T. Q. Nguyen, J. Petkovi , P. Dangla, and V. Baroghel-Bouny, “Modelling of coupled ion and moisture transport in porous building materials,” *Constr. Build. Mater.*, vol. 22, no. 11, pp. 2185–2195, Nov. 2008.
- [108] G. W. C. Kaye and T. M. Laby, *Tables of Physical and Chemical Constants*. Harlow: Longman, 1973.
- [109] R. B. Bird, W. E. Stewart, and E. N. Lighfoot, *Transport Phenomena*. New York: J. Wiley, 2002.
- [110] H. Ni, A. K. Datta, and K. E. Torrance, “Moisture transport in intensive microwave heating of biomaterials: a multiphase porous media model,” *Int. J. Heat Mass Transf.*, vol. 42, pp. 1501–1512, 1999.



- [111] H. S. Carslaw and J. C. Jaeger, *Conduction of Heat in Solids*. London: Oxford University Press, 1959.
- [112] P. Boeraeve, "Introduction To The Finite Element Method," Liege, 2010.
- [113] R. W. Lewis, W. K. Sze, and H. C. Huang, "Some novel techniques for the finite element analysis of heat and mass transfer problems," *Int. J. Numer. METHODS Eng.*, vol. 25, pp. 611–624, 1988.
- [114] S. Chemkhi and F. Zagrouba, "Development of a Darcy-flow model applied to simulate the drying of shrinking media," *Brazilian J. Chem. Eng.*, vol. 25, no. 3, pp. 503–514, 2008.
- [115] J. F. Siau, *Flow in Wood*. New York: Springer, 1986.
- [116] J. A. Mardini, A. S. Lavine, and V. K. Dhir, "Heat and mass transfer in wooden dowels during a simulated fire: an experimental and analytical study," *Int. J. Heat Mass Transf.*, vol. 39, no. 13, pp. 2641–2651, Sep. 1996.
- [117] Z. Przesmycki and C. Strumillo, "The Mathematical Modelling of Drying Process based on Moisture Transfer Mechanisme," *Dry. '85*, pp. 126–134, 1985.
- [118] M. E. Katekawa and M. A. Silva, "A Review of Drying Models Including Shrinkage Effects," *Dry. Technol.*, vol. 24, no. 1, pp. 5–20, Feb. 2006.
- [119] L. Bennamoun, Z. Chen, A. A. Salema, and M. T. Afzal, "Moisture diffusivity during microwave drying of wastewater sewage sludge," in *2014 ASABE and CSBE/SCGAB Annual International Meeting*, 2014.
- [120] S. Kowalski, G. Musielak, and J. Banaszak, "Heat and mass transfer during microwave-convective drying," *AIChE J.*, vol. 56, no. 1, pp. 24–35, 2010.
- [121] A. J. J. Van Der Zanden and A. M. E. Schoenmakers, "The influence of sorption isotherms on the drying of porous materials," *Int. J. Heat Mass Transf.*, vol. 39, no. 11, pp. 2319–2327, 1996.

- [122] A. H. Nissan, H. H. George, and T. V. Bolles, "Mechanism of drying thick porous bodies during the falling-rate period: III. Analytical treatment of macroporous systems," *AIChE J.*, vol. 6, no. 3, pp. 406–410, 1960.
- [123] S. J. Kowalski, "Continuous Thermohydromechanical Model using the Theory of Mixtures," in *Modern Drying Technology*, Volume 1., E. Tsotsas and A. S. Mujumdar, Eds. Weinheim: Wiley VCH Verlag GmbH & Co. KGaA, 2007, pp. 125–154.